AGU PUBLICATIONS

JGR

Journal of Geophysical Research: Solid Earth

RESEARCH ARTICLE
10.1002/2016JB013848

Key Points:
- A new model of seismic crustal structure of the North China Craton
- Westward increase in thickness of all crustal layers, with no trend for average V_p and the *Pn* velocities
- Topography in this region is mostly controlled by the crustal heterogeneity

Correspondence to:
B. Xia, H. Thybo, I. M. Artemieva,
bixi@ign.ku.dk;
thybo@geo.uio.no;
irina@ign.ku.dk

Citation:
Xia, B., H. Thybo, and I. M. Artemieva (2017), Seismic crustal structure of the North China Craton and surrounding area: Synthesis and analysis, *J. Geophys. Res. Solid Earth*, *122*, doi:10.1002/2016JB013848.

Received 14 DEC 2016
Accepted 26 APR 2017
Accepted article online 27 APR 2017

Seismic crustal structure of the North China Craton and surrounding area: Synthesis and analysis

B. Xia[1,2], H. Thybo[3,4], and I. M. Artemieva[1]

[1]Geology Section, Department of Geosciences and Natural Resource Management, University of Copenhagen, Copenhagen, Denmark, [2]State Key Laboratory of Geological Processes and Mineral Resources, School of Earth Science, China University of Geosciences, Wuhan, China, [3]Eurasia Institute of Earth Sciences, Istanbul Technical University, Istanbul, Turkey, [4]Centre for Earth Evolution and Dynamics, University of Oslo, Oslo, Norway

Abstract We present a new digital model (NCcrust) of the seismic crustal structure of the Neoarchean North China Craton (NCC) and its surrounding Paleozoic-Mesozoic orogenic belts (30°–45°N, 100°–130°E). All available seismic profiles, complemented by receiver function interpretations of crustal thickness, are used to constrain a new comprehensive crustal model NCcrust. The model, presented on a 0.25° × 0.25°grid, includes the Moho depth and the internal structure (thickness and velocity) of the crust specified for four layers (the sedimentary cover, upper, middle, and lower crust) and the *Pn* velocity in the uppermost mantle. The crust is thin (30–32 km) in the east, while the Moho depth in the western part of the NCC is 38–44 km. The Moho depth of the Sulu-Dabie-Qinling-Qilian orogenic belt ranges from 31 km to 51 km, with a general westward increase in crustal thickness. The sedimentary cover is 2–5 km thick in most of the region, and typical thicknesses of the upper crust, middle crust, and lower crust are 16–24 km, 6–24 km, and 0–6 km, respectively. We document a general trend of westward increase in the thickness of all crustal layers of the crystalline basement and as a consequence, the depth of the Moho. There is no systematic regional pattern in the average crustal V_p velocity and the *Pn* velocity. We examine correlation between the Moho depth and topography for seven tectonic provinces in the North China Craton and speculate on mechanisms of isostatic compensation.

1. Introduction

Detailed knowledge of crustal structure may be obtained from a combination of geophysical observations, experimental petrology at high temperature and pressure, and studies of exposed crustal sections and crustal xenoliths carried in basalts and kimberlites. Geophysical observations (seismic, gravity, and borehole data) provide the means of probing the generally inaccessible deep crust over large areas. Recently, several crustal structure models, constrained by seismic studies in continental areas, have been presented for Eurasia [*Artemieva and Thybo*, 2013; *Cherepanova et al.*, 2013] and Asia [*Stolk et al.*, 2013].

A series of destructive earthquakes in North China has drawn increased attention to the crustal structure of the region. Numerous wide-angle seismic profiles [*Li et al.*, 2006; *Teng et al.*, 2013; *Zhang et al.*, 2011] provide observations of the crustal/mantle lithospheric structure of this region (Figure 1a). A total of 37 seismic reflection/ refraction profiles with a total length of ~18,000 km was acquired from 1976 to 1993. Ten profiles (1–10; blue lines in Figure 1a) were chosen to form part of four transects in a program of the Global Geoscience Transects, and they form the basis for the global model CRUST 1.0 for this region. Between 1998 and 2005, several short seismic profiles were acquired for academic research. After 2008, long-range (>1000 km) seismic profiles across the whole North China Craton (pink lines in Figure 1a) provided new observations of the seismic velocity structure of the crust and the uppermost mantle in the region. Further high-resolution deep seismic reflection profiling by the SinoProbe Program (Profiles 47 and 48 in Figure 1a) provides reliable lithosphere-scale information for the northern and southern margin of the North China Craton.

More than 30,000 km of 41 refraction/wide-angle reflection profiles across the whole of China have early been used to constrain the Moho depth (Figure 1b and Table 1) [*Li and Mooney*, 1998]. An updated contour map of the crustal thickness constrained by 90 refraction/wide-angle reflection profiles (total length of about 60,000 km) was reported recently (Figure 1b and Table 1) [*Li et al.*, 2006]. The interpreted results of 114 seismic

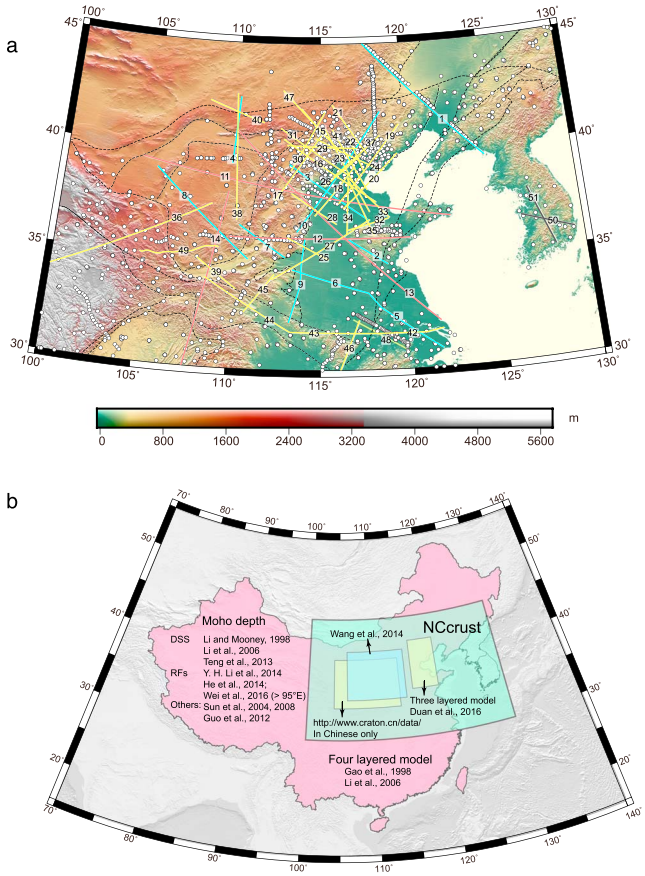

Figure 1. (a) Topography and deep seismic profiles used to constrain NCcrust (Black lines: geological boundary; blue lines: profiles 1–10 in Table 1; pink lines: profiles 11–14 in Table 1; yellow lines: profiles 15–48 in Table 1; white dots: Receiver function interpretations for the Moho depth). (b) Coverage of the China continent by models of the Moho depth (deep seismic sounding: [*Li and Mooney*, 1998; *Li et al.*, 2006; *Teng et al.*, 2013]; receiver functions: [*Y. H. Li et al.*, 2014; *He et al.*, 2014; *Wei et al.*, 2016]; tomography: [*Sun et al.*, 2004, 2008; Gravity: *Guo et al.*, 2012]; and crustal structure [*Gao et al.*, 1998; *Li et al.*, 2006; *Duan et al.*, 2016].

profiles allowed for comparing the average *P* wave velocity and the Moho depths for tectonic provinces (Figure 1b and Table 1) [*Teng et al.*, 2013]. A high-resolution Moho depth map of China was also derived from receiver function data analysis (Figure 1b) [*He et al.*, 2014; *Y. H. Li et al.*, 2014; *Wei et al.*, 2016]. A layered model of shear wave velocity of the crust and uppermost mantle velocity of China and surrounding area was constrained by body wave tomography (Figure 1b) [*Sun et al.*, 2004, 2008]. *Guo et al.* [2012] constrain a new Moho depth model including information from the Bouguer gravity anomaly. Based on analysis of seismic profiles, four-layered (upper, middle, lower, and lowermost crust) crustal models were obtained for different tectonic units in China (Figure 1b and Table 1) [*Gao et al.*, 1998; *Li et al.*, 2006]. Most recently, a three-layer (sediments, upper and lower crust) model (HBCrust1.0) constrained by 42 seismic profiles on a grid of 0.25° × 0.25° × 2 km became available for a small area (112° – 120°E, 36° – 42°N) (Figure 1b and Table 1) [*Duan et al.*, 2016] (also see http://www.craton.cn/data Chinese webpage of HBCrust1.0).

This study presents a new crustal model (NCcrust) for the whole North China Craton and the surrounding regions. Compared to other regional crustal models,

1. NCcrust covers a larger area (Figure 1b), which includes the Phanerozoic Sulu-Dabei-Qinling-Qilian orogenic belt in the south and the Precambrian North China Craton (Figure 2). The NCcrust is available digitally on a uniform grid 0.25° × 0.25° for the region 100° – 130°E, 30° – 45°N.
2. NCcrust includes information on the internal structure of the crust (V_p velocity and thickness) for four crustal layers (sedimentary cover, upper crust, middle crust, and lower crust) and the *Pn* velocity in the uppermost mantle, based on all available seismic profiles and receiver function results.

Journal of Geophysical Research: Solid Earth

10.1002/2016JB013848

Table 1. Summary of Crustal Model for China[a]

Crustal Models	LM98	T13	L14	H14	W16	S04	S08	G12	W14	L06	G98	D16	NCcrust
Area	China	China	China	China	China	China	China	China	102–116°E	China	China	112–120°E	100–130°E
					>95°E				32–42°N			36–42°N	30–45°N
Model parameters													
Moho depth	seismic profiles data		RF	RF	RF	tomography		gravity	RF	seismic profiles data			seismic profiles data + RF
Sedimentary cover	No	No	No	No	No	No	No	No	No	No	No	No	Yes
Crystalline crust													
Thickness	No	No	No	No	No	No	No	No	No	average of different blocks		No	Yes
V_p	No	No	No	No	No	No	No	No	No	No	No	Yes	Yes
Pn velocity	No	No	No	No	No	Yes	No	No	Yes	No	No	No	Yes
Digital form	No	No	No	No	No	No	No	No	No	No	No	No	Yes

[a] RF: Receiver function. LM98: *Li and Mooney*, 1998; T13: *Teng et al.*, 2013; L14: *Y. H. Li et al.*, 2014; H14: *He et al.*, 2014; W16: *Wei et al.*, 2016; S04: *Sun et al.*, 2004; S08: *Sun et al.*, 2008; G12: *Guo et al.*, 2012; L06: W14: *C. Y. Wang et al.*, 2014; *Li et al.*, 2006; G98: *Gao et al.*, 1998; D16: *Duan et al.*, 2016; NCcrust: our study.

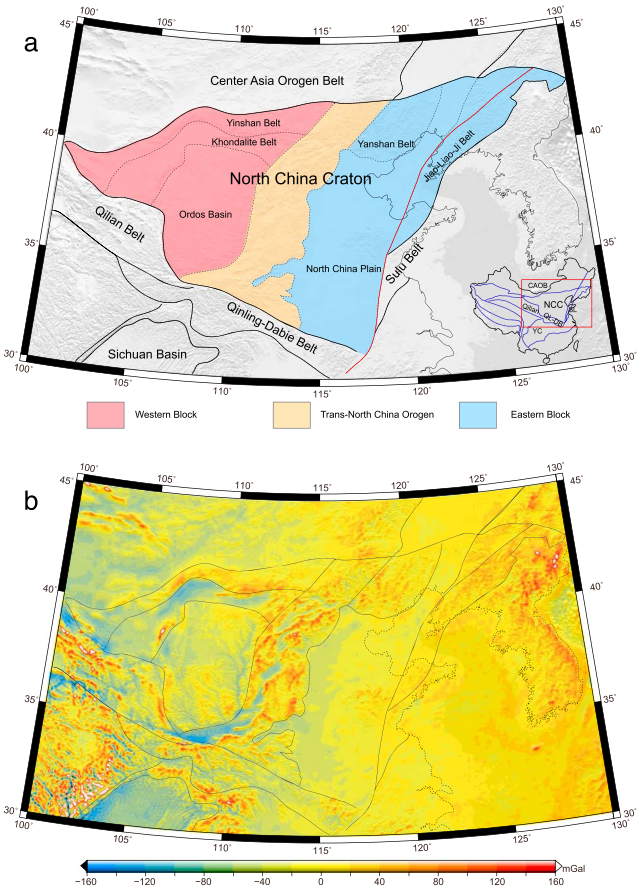

Figure 2. (a) Geological map of the North China Craton and adjacent region. CAOB: the Central Asian Orogenic Belt; NCC: the North China Craton; WB: the Western Block, EB: the eastern block, QL-DB: the Qinling-Dabie Belt, SL: the Sulu Belt, YC: the Yangtze Craton Geological boundaries are after *Zheng et al.* [2013] with modifications. (b) Free-air gravity anomaly map of the NCC. Data from EGM-2008.

3. NCcrust is based on seismic data from the region, and we emphasize that it does not include gravity data, such that the model is suitable for gravity studies such as calculation of mantle gravity and density [*Herceg et al.*, 2016; *Kaban et al.*, 2003; *Yegorova et al.*, 2007].
4. The Eastern Block has a relatively shallow Moho of unclear origin, and we provide possible explanations based on our model.
5. Based on NCcrust, regional correlation between Moho depth and topography for different tectonic provices were examined. In addition, we speculate on the contributions to topography for each tectonic provine and the mechanisms of isostatic compensation.

2. Geological Background

The study area comprises the North China Craton and the surrounding orogenic belts (Figure 2a). This area has experienced a complicated tectonic evolution which we briefly review below.

2.1. Orogenic Belts

The WWN-EES trending 300 km wide and 1200 km long [*Tseng et al.*, 2009; *C. Y. Wang et al.*, 2005] Qilian orogenic belt constitutes the main part of the northeastern margin of the Tibetan Plateau. Geological, petrological, and geochemical studies suggest that the Qilian Belt records the history of the spreading, subduction, and closure of the Qilian Ocean; collision between the southwestern part of the North China Craton and the Qaidam blocks (in the northern Tibetan Plateau); and postcollisional tectonic evolution from ~550 Ma to ~400 Ma 2013. The complex geodynamic evolution and its lack of isostasy equilibrium of the Qilian Belt is reflected in a highly heterogeneous free-air gravity anomaly which ranges from −150 mGal to +150 mGal (Figure 2b).

The Qinling-Dabie-Sulu orogenic belt is a 2000 km long Mesozoic [*Li et al.*, 1993] high pressure-ultra high pressure (UHP) metamorphic belt. It records the multistage evolution processes of arc-terrane accretion, arc-continent, and continent-continent collisions from ~430 Ma (the Ordovician) to ~215 Ma (the Triassic) between the North China Craton and the Yangtze Block. It is separated into two terranes by the Mesozoic Tan-Lu (Tancheng-Lujiang) fault which separates the Qinling-Dabie Belt in the west from the Sulu Belt in the east. The orogen is close to isostatic equilibrium with typical values of free-air gravity anomalies of ±20 mGal (Figure 2b), which show a significant scatter in the western part of the orogeny.

2.2. The North China Craton

The North China Craton, covering a triangular-shaped area of 1,500,000 km^2, is bounded to the southwest and north by the early Paleozoic Qilian Orogen and the late Paleozoic Central Asia Orogen, respectively. It is separated from the Yangtze Craton in the south and east by the Qinling-Dabie-Sulu UHP metamorphic belt. The North China Craton was traditionally considered to consist of Precambrian (Archean to Paleoproterozoic) basement overlain by later (Proterozoic to Cenozoic) sedimentary covers. It is generally considered to be formed by three discrete crustal blocks, namely, the Eastern Block, the Western Block, and the intervening Trans-North China Orogen (TNCO). The transition from the TNCO to the eastern block is marked by a sharp drop in topography from nearly 2 km to close to 100 m, and it approximately coincides with the westward extent of Mesozoic subduction. The Eastern Block which includes the North China Plain, the Yanshan Belt, and the Jiao-Liao-Ji Belt is characterized by high surface heat flow of ~64 mW/m^2 [*He*, 2015] and has been strongly affected by a thermal event between the Paleozoic and the late Cenozoic. And the Western Block which includes the Ordos Basin, the Yinshan Belt, and the Khondalite Belt has lower heat flow (>50 mW/m^2) [*He*, 2015] and is considered to be the most stable part of the North China Craton. There is no geological evidence for significant deformation within the Western Block of the North China Craton, which also lacks big earthquakes.

The oldest rocks in the North China Craton have ages of 3.8–3.6 Ga [*Liu et al.*, 1992; *Song et al.*, 1996]. Published zircon Hf and whole-rock Nd isotopic data from Neoarchean rocks indicate that the major crustal growth in the NCC took place at 2.8–2.7 Ga [*Geng et al.*, 2012; *Wu et al.,* 2005b] followed by 2.6–2.5 Ga remelting or differentiation of the crust. The North China Craton is traditionally considered to be finally assembled by Paleoproterozoic time and to be stable until the eruption of kimberlites in the Paleozoic [*Q. L. Li et al.*, 2011]. Later, the craton has been reactivated or decratonized by the Mesozoic Pacific subduction, with tectonic uplift and basin development [*Wu et al.*, 2005a]. These processes may also have produced strong lateral heterogeneities in the lithosphere structure [*Chen*, 2012; *Chen et al.*, 2014].

The Ordos Basin, located in the western North China Craton with an area of over 250,000 km^2, is a large Mesozoic intracontinental basin. It is surrounded by the Trans-North China Orogen in the east, the Khondalite Belt in the north, and the Qilian fold system in the southwest. This basin with a Neoarchean basement experienced subsidence and sedimentation in the Paleozoic, with further basin formation in Mesozoic and Cenozoic. The basin is close to isostatic equilibrium, as indicated by near-zero, weakly negative free-air gravity anomalies (Figure 2b). The Yinshan Belt across at the northwestern edge of the NCC contains extensive exposures of Archean rocks and is also close to isostatic equilibrium (Figure 2b). The nearly east-west trending Paleoproterozoic Khondalite Belt, located between the Ordos Basin and the Yinshan belt, is a collisional belt that together with the Yinshan and the Ordos Basin forms the Western Block of the NCC since ~1.95 Ga [*Zhao and Zhai*, 2013]. Most of the Western Block is tectonically stable over more than 2.5 Ga [*Chen et al.*, 2009], but significant deviation from regional isostasy is typical at the Khondalite Belt (free-air gravity anomaly range from −100 mGal to +100 mGal; Figure 2b).

The North China Plain covers approximately 310,000 km^2. It is located between the Qingling-Dabie-Sulu Orogenic belt to the south and the Yanshan Belt to the north, the Trans-North China Orogen to the west, and the Su-Lu belt to the east. The plain developed on Archean granulites and Paleoproterozoic greenschists, and it is filled with Paleozoic to Cenozoic sedimentary rocks. The EW trending Yanshan Belt is located in the northeastern part of the North China Craton and was formed by collision and extension in the Mesozoic. The Jiao-Liao-Ji Belt underwent rifting to form an incipient ocean that was closed at Paleoproterozoic (~1.9 Ga) through subduction and collision [*Zhao and Zhai*, 2013]. All three tectonic provinces are at near-isostatic equilibrium with free-air gravity anomalies typically ranging from −20 mGal in the North China Plain to +20 mGal in the Jiao-Liao-Ji Belt (Figure 2b).

The Western Block collided with the exotic Eastern Block along the 100–300 km wide and 1200 km long SW-NE trending Trans-North China Orogen in the early Proterozoic (~1.85 Ga). The Trans-North China Orogen (TNCO) consists of both high-pressure granulites and low-grade granite-greenstone complexes which contain many classic indicators of collision tectonics. This belt is well recognized by the heterogeneous pattern of free-air gravity anomalies that vary locally between −100 mGal and +100 mGal with an average value of around zero (Figure 2b).

3. Seismic Data on the Crustal Structure

3.1. Database

NCcrust is constrained by all available deep sounding reflection/refraction seismic profiles in North China with a total length of more than 23,000 km (Figure 1a and Table 2). We also use receiver function analysis results (white dots in Figure 1a) [*He et al.*, 2014; *Y. H. Li et al.*, 2014; *Wei et al.*, 2016] to constrain the Moho depth, whereas the internal structure and crustal and *Pn* velocities are based on deep sounding reflection/refraction seismic profile only.

In case of multiple interpretations for the same seismic profile (e.g., Profile 10, the Shijiazhuang-Kalaqin, interpreted by *Sun et al.* [1985] and by *S. J. Wang et al.* [2005]) we preferred the latest one, since recent interpretations are usually of a higher quality. For the Wendeng-Alashan profile (Profile 11 in Figure 1a) [*Jia et al.*, 2014; *Tian et al.*, 2014], we use the interpretation by the data acquisition group. If two or more profiles cross the same area (e.g., the Capital area), we use the most recent (after 2000) data acquisition and interpretation.

To constrain the Moho depth (Figure 3a), in addition to reflection/refraction seismic profiles, three receiver function databases are used for establishing our model [*He et al.*, 2014, *Y. H. Li et al.,* 2014, *Wei et al.*, 2016]. To decrease the uncertainty related to the receiver function interpolation method, we carefully compared the result from these three models. For the same station, if the difference between two or three interpretations of Moho depth is less than 3 km, we use the average. If the difference between all three interpretations of Moho depth is >3 km, we do not use the result of that station.

In most places, there is a close match in between the Moho depth based on receiver function results and reflection/refraction profiles results (Figure 3b). For example, *Y. H. Li et al.* [2014] compare the difference in the Moho depth in the North China Craton between different methods and show that it is less than 2 km in most of the area. This kind of match was also found in Southern Africa [*Durrheim and Green*, 1992; *Niu and James*, 2002], Western Superior Craton [*Angus et al.*, 2009; *Cook et al.*, 2010], and Norway [*Stratford and Thybo*, 2011; *Frassetto and Thybo*, 2013].

3.2. Structure of the Database

Based on typical V_p velocities, we subdivide the crustal structure into four layers:

1. Sedimentary cover: $V_p < 5.8$ km/s
2. Upper crust: 5.8 km/s–6.4 km/s
3. Middle crust: 6.4 km/s–6.8 km/s
4. Lower crust: 6.8 km/s–7.3 km/s

These values for the lower crust are in agreement with laboratory measurements of *P* wave velocities in granulites from the North China Craton with V_p values of 6.8 km/s–7.3 km/s [*Gao et al.*, 2000] and in retrograde eclogite from a drill core of the Chinese Continental Scientific Drilling Project (the Su-Lu Orogenic belt) with *P* wave velocity of 6.8 km/s–7.1 km/s [*Sun et al.*, 2012]. They are also in agreement with crustal models for other continental regions [*Artemieva and Thybo*, 2013; *Cherepanova et al.*, 2013] as well as global models such as CRUST 1.0 [*Laske et al.*, 2013]. We note that some places (e.g., Ordos Basin) have a 5 km thick layer with a *P* wave velocity of 6.7 km/s. With our definition this forms part of the middle crust, whereas it will be part of the lower crust if the limit is at 6.7 km/s as some authors have defined it.

Our database is based on point data constrained by digitization along seismic profiles with a lateral step not larger than 50 km and more dense sampling in regions with a fast change in V_p crustal structure. Therefore, the areal coverage of the NCcrust model is nonuniform. In order to present a regional crustal structure on a uniform grid, our digital regional maps are produced by interpolation.

All maps of the crustal structure are produced by the kriging method with an interpolation radius of 1°. The largest gap without seismic data coverage in our study area is <2°in the Western Block which supports the choice of an interpolation radius of 1°. The interpolation parameters are chosen after a comparison

Table 2. Summary of Seismic Profiles

No.	Profile Name	Length (km)	Reference
1	Dongwuzhumuqinqi-Donggou	960	*Lu and Xia* [1993]
2	Lianyungang-Lingyi-Sishui	328	*Liu et al.* [1991] and *G. J. Wang et al.* [2007]
3	Zhucheng-Dingxian-Tuoketuo	530	*Liu et al.* [1991]
4	Xi'an-Yan'an-Baotou-Baiyunebo	1120	*Chinese State Seismological Bureau (CSSB)* [1988]
5	Fengxian-Fuliji	570	*Zhang et al.* [1988] and *Bai and Wang* [2006]
6	Lingbi-Zhengzhou	502	*CSSB* [1988]
7	Zhengzhou-LingFen-Jingbian	633	*CSSB* [1988]
8	Zhengzhou-Yinchuan (west)	680	*CSSB* [1988]
9	Suixian-Anyang	480	*Hu et al.* [1986]
10	Shijiazhuang-KaLaqinqi	746	*Sun et al.* [1985] and *S. J. Wang et al.* [2005]
11	Wendeng-Alashan	1500	*Jia et al.* [2014], *Tian et al.* [2014], and *S. J. Wang et al.* [2014]
12	Zhucheng-Yichuan	1019	*S. L. Li et al.* [2011]
13	Dafeng-Baotou		*Duan et al.* [2015]
14	Chongqing-Yulin		*Teng et al.* [2014]
15	Beijing-Zhangjiakou-Huade	300	*Zhao et al.* [2005]
16	Haixing-Yangyuan-Fengzheng	579	*J. S. Zhang et al.* [1997]
17	Taiyuan-Xuanhua	550	*Zhao et al.* [2006]
18	Renxian-Hejian-Wuqing	431	*Chinese State Seismological Bureau (CSSB)* [1986]
19	Cangzhou-Tianjin-KaLaqinzuoyi	510	*CSSB* [1986]
20	Dezhou-Qinhuangdao	587	*CSSB* [1986]
21	Baigezhuang-FengNing-Zhenglanqi	407	*CSSB* [1986]
22	Tanggu-Sanhe-Miyun	220	*CSSB* [1986]
23	Yanshan-Daxin-Yanqing	476	*S. Wang et al.* [2005]
24	Ninghe-Beijing-Zhuolu	450	*Zhao et al.* [1999]
25	Heze-Lingzhou-Changzhi	304	*Jia and Liu* [1991] and *Ren et al.* [1992]
26	Anguo-Yongqin-Zunghua	350	*Chinese State Seismological Bureau (CSSB)* [1986]
27	Zhengzhou-Jinan	600	*Zhang et al.* [1994]
28	Taian-Longyao-Xinxian	480	*Chinese State Seismological Bureau (CSSB)* [1986]
29	Beijing-Huailai-Fengzhen	342	*Zhang et al.* [1996] and *S. Wang et al.* [2005]
30	Fanzhi-Huailai-Taipushiqi	302	*Nie et al.* [1998] and *Lai et al.* [2004]
31	Wenan-Weixian-Chayouzhongqi	420	*C. K. Zhang et al.* [1997]
32	Qihe-Zhangqiu-Shouguang	240	*Chinese State Seismological Bureau (CSSB)* [1995]
33	Shouguang-Zhanhua-Wenan	291	*CSSB* [1995]
34	Wenan-Dezhou-Qihe	290	*CSSB* [1995]
35	Yiyuan-Lelin-Dacheng	315	*CSSB* [1995]
36	Maqin-Lanzhou-Jingbian	941	*Li et al.* [2002]
37	Anxin-Xianghe-Kuancheng	320	*Wang et al.* [2004] and *Zhang et al.* [2011]
38	Yanchuan-Baotou-Manladu	680	*Teng et al.* [2010]
39	Danfeng-Xian-Binxian		*CSSB* [1986]
40	Damo-Baiyunebo-Baxin		*CSSB* [1986]
41	Tianjin-Beijing-Chicheng	320	*S. J. Wang et al.* [2007]
42	Maanshan-Qidong	300	*Teng* [1985]
43	Suixian-Maanshan	500	*Zheng and Teng* [1989]
44	Suixian-Xian	400	*Ding et al.* [1987]
45	Yichuan-Shiyan	280	*Cao et al.* [1994]
46	Zhuangmu-Zhanggongdu	420	*Dong et al.* [1998] and *Wang et al.* [1997]
47	Huailai-Suniteyouqi	453	*W. H. Li et al.* [2014]
48	Lixin-Yixing	450	*Xu et al.* [2014]
49	Ordos-Liupanshan	500	*Li* [2013]
50	KCRT2002	250	*Cho et al.* [2006]
51	KCRT2004	340	*Cho et al.* [2013]

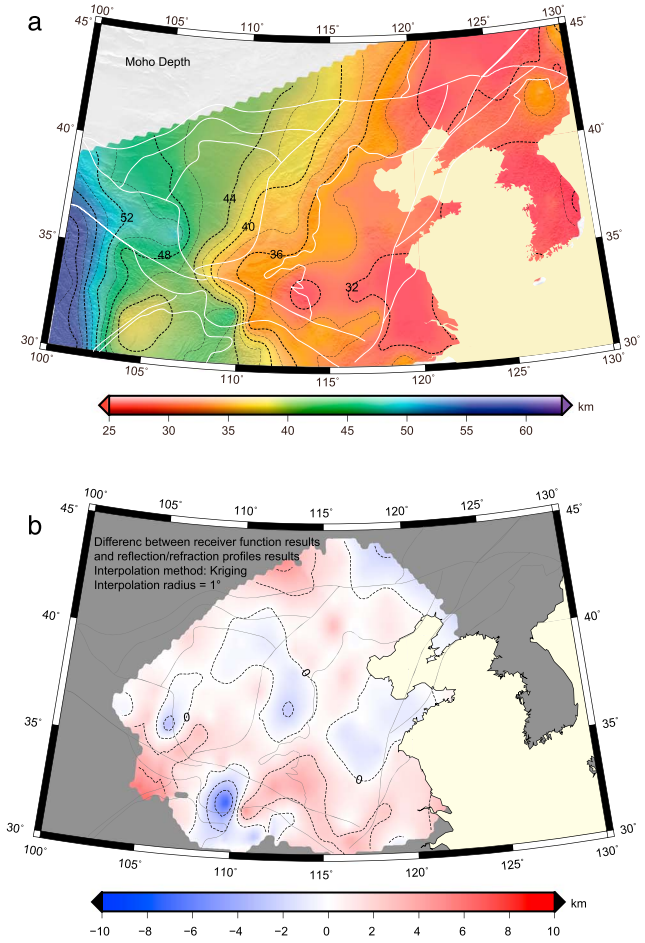

Figure 3. (a) Depth of Moho (below sea level). (b) Difference between values from seismic profiles and receiver function studies. Color scales are the same as in Figures 4 and 5.

between different interpolation radii and gridding methods (Figures 3 and 4) in order to minimize deviations of interpolated values from the seismic data and to avoid bull's-eye anomalies and similar artifacts from small interpolation radius (Figure 4a). In most regions the uncertainties of interpolation with different radii are <2 km for the Moho depth which is comparable to the resolution of the seismic methods, but locally, in two regions with very sparse data they may be up to 6 km as indicated by the calculated differences between results based on different interpolation methods (Figures 4b and 4c). We note that even these interpolation differences are significantly smaller than the difference in the Moho depth between the NCcrust model and the global CRUST1.0 model and a regional receiver function (RF)-based crustal model (Figure 5).

4. Analysis of the NCcrust: General Patterns and Regional Variations

4.1. Precambrian Crust of the North China Craton

4.1.1. Moho Depth

The NCcrust model shows that the Archean crust of the North China Craton is strongly heterogeneous and that generally the crust thickens from east to west (Figure 3). The Moho is shallow in the east (30 km) and deep in the west (up to ~55 km) close to the edge of the Tibetan Plateau. A relatively thin crust (<32 km) is also observed in the southern part of TNCO, as compared to the surrounding areas (Figure 3).

Reworked Archean crust with a thickness of less than 36 km (mostly 32–34 km) is typical of the entire Eastern Block (including the North China Plain, the Yanshan Belt, and the Paleoproterozoic Jiao-Liao-Ji Belt. It is therefore much thinner than the global average of 40–42 km for cratonic crust [*Mooney et al.*, 1998].

The Paleoproterozoic collision of the Western and Eastern blocks formed the Trans-North China Orogen (TNCO) at ~110°–118°E. Similar to the regional pattern, the Moho depth shows an east-west increasing trend

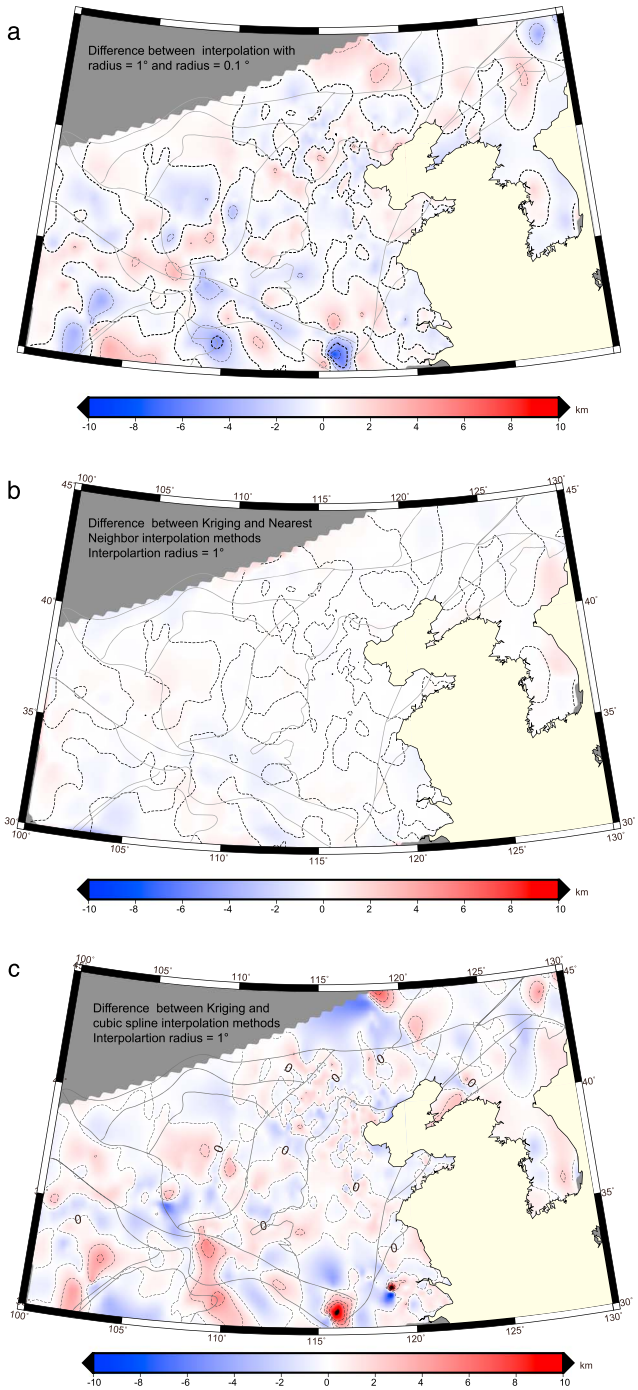

Figure 4. (a) Uncertainty related to interpolation radius: difference between the Moho depth models based on interpolation radius = 1°and radius = 0.1°. (b) Uncertainty associated with interpolation method: Moho depth map by nearest neighbor and Kriging interpolation method. (c) Difference between Kriging and cubic spline interpolation methods. Color scale is the same in Figures 4a–4c and the same as in Figures 3 and 5.

even in this narrow orogenic belt and on average the eastern part is 3–5 km shallower (~34–36 km) than the western part (~38–41 km). It is remarkable that while the crust is thin (<40 km) in most of the TNCO, the topography is relatively high (1–2 km).

The average Moho depth in the Ordos Basin is 44.0 ± 3.0 km. The range of the Moho depth variation is extremely large, from ~35 km in the east to 47 km in the west. Two interfaces were determined beneath the eastern margin of the Ordos Basin by virtual deep seismic sounding and teleseismic waveform technique

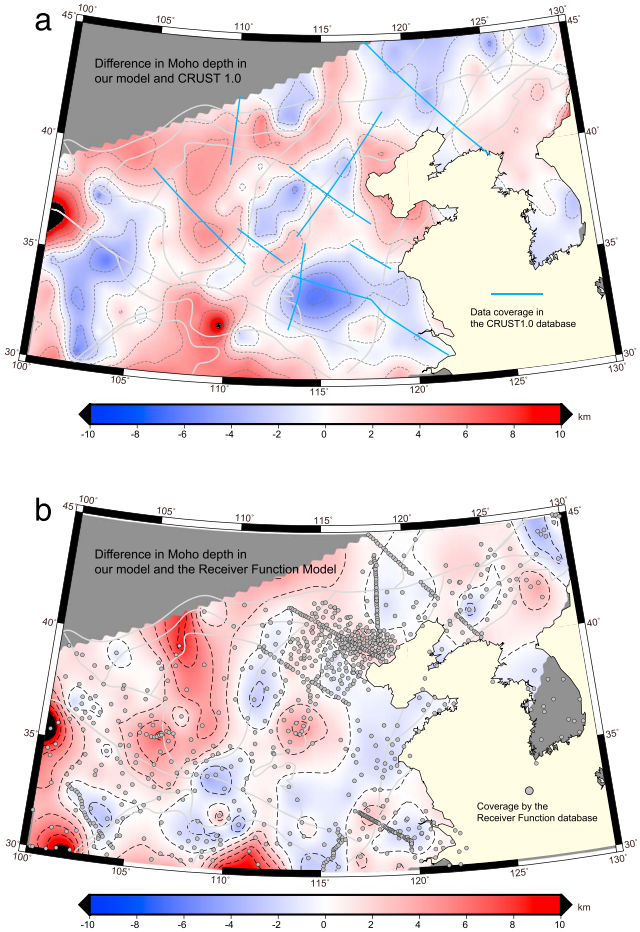

Figure 5. Maps of difference between Moho depth in NCcrust and (a) CRUST 1.0 [*Laske et al*., 2013]. (b) Receiver function studies [*He et al*., 2014]. Color scales are the same as in Figures 3 and 4.

together with the receiver function method [*Yu et al.*, 2012]. One interface is at ~40 km depth and the other at ~60 km depth. Based on absolute seismic velocities, these authors interpret the deeper interface as the Moho and the shallower one as the Conrad discontinuity. Seismic reflection and refraction profiles across the Ordos Basin also suggest the presence of seismic interfaces at ~40 km and ~60 km depths beneath the northeastern Ordos Basin [*Teng et al.*, 2010]. However, these authors interpret the shallower interface as the Moho because the *P* wave velocity increases from 6.8 km/s to 8.0 km/s at the ~40 km deep interface and from 8.0 km/s to 8.5 km/s at ~60 km depth. Because the velocities observed by refraction seismology have less uncertainty than from the receiver function method, we favor the interpretation that the Moho is located at a 40 km depth. At the same location, double interfaces were observed in receiver functions from teleseismic events at different azimuths, and the shallower interface at 40 km depth was interpreted as the Moho [*He et al.*, 2014], in agreement with our interpretation. Further, the most recent seismic reflection profile (Profile 11 in Figure 1a) [*Jia et al.*, 2014; *Tian et al.*, 2014] and the crustal shear wave velocity structure from ambient noise tomography [*Cheng et al.*, 2013] also suggest that the Moho depth is ~40 km. Seismic refraction study of the upper mantle beneath the Ordos Basin shows a relatively weak reflectivity in the *P* wave section at 60 km depth, and the most recent interpretation of this profile (Profile 38 in Figure 1a) does not include any reflector at ~60 km depth [*Zhang et al.*, 2014]. We therefore consider the ~40 km deep interface as the Moho in the NCcrust model for the Ordos Basin.

We compare the Moho depth distribution in the NCcrust model with other regional and global models (Figures 5 and 6). The RF model which has been compiled by [*He et al.*, 2014; *Y. H. Li et al.*, 2014; *Wei et al.*, 2016] shows similar variations in the Moho depth in the NCC, as a gravity-derived model [*Guo et al.*, 2012] and a tomographic model [*Sun et al.*, 2004, 2008]. It is not surprising that all models show a similar average Moho depth in most parts of the North China Craton (Figures 5 and 6), where the seismic data coverage is good.

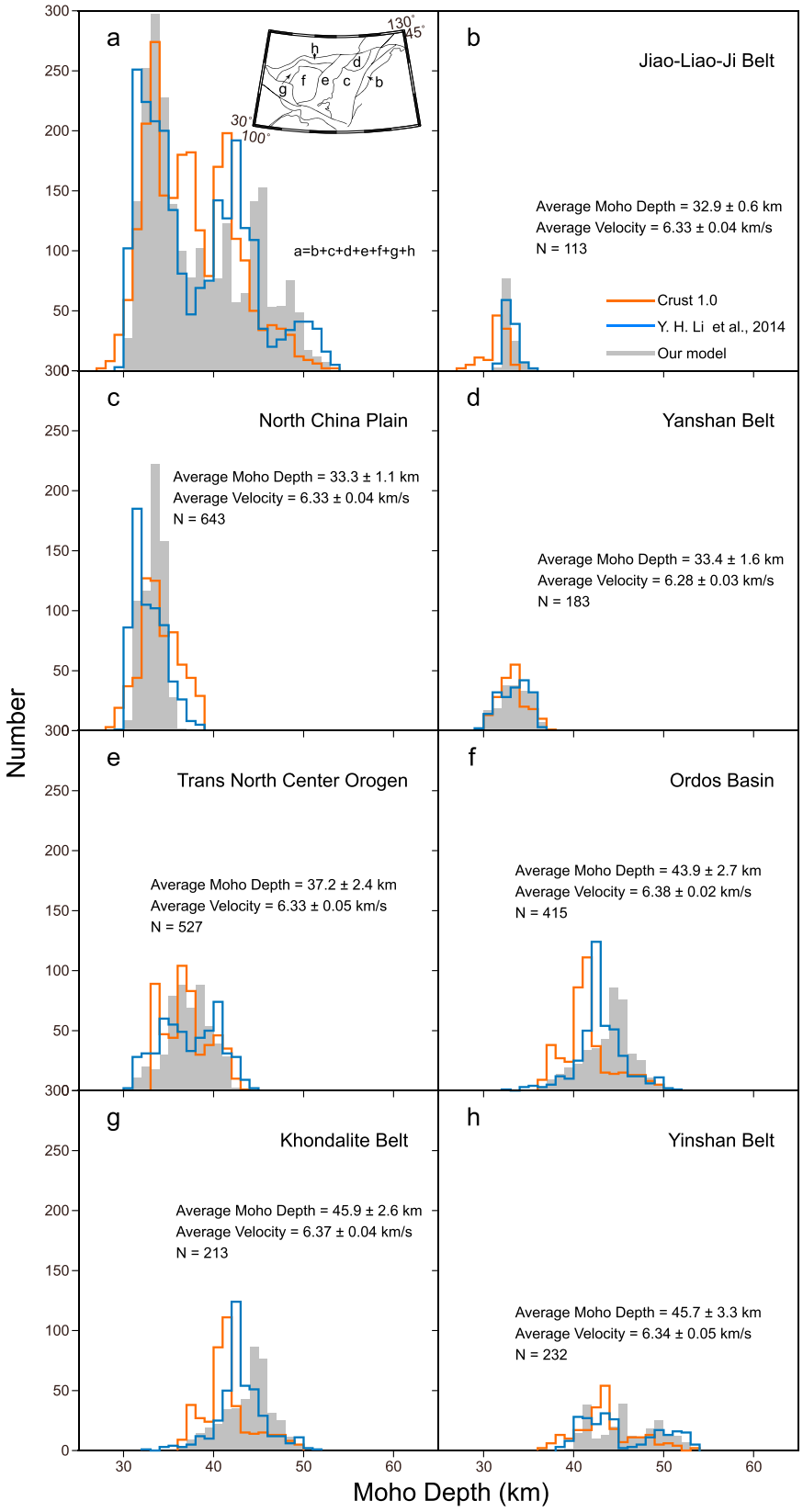

Figure 6. (a–h) Histograms of the Moho depth for different parts of the North China Craton in comparison with the data from (Figure 6a) CRUST 1.0 [*Laske et al.*, 2013] and (Figure 6b) receiver function studies [*He et al.*, 2014]. See Figure 5 for details.

Journal of Geophysical Research: Solid Earth

10.1002/2016JB013848

Table 3. Typical Crustal Structure in Different Tectonic Province (σ Denotes the Standard Variation)

	Moho Depth (km)		*Pn* Velocity (km/s)		Upper Crust				Middle Crust				Lower Crust			
					Thickness (km)		Velocity (km/s)		Thickness (km)		Velocity (km/s)		Thickness (km)		Velocity (km/s)	
	Average	σ	Average	σ	Average	σ	Average	σ	Average	σ	Average	σ	Average	σ	Average	σ
North China Craton																
Average	38.5	5.6	8.04	0.06	21.1	2.4	6.14	0.05	13.0	3.6	6.58	0.04	2.9	1.7	6.90	0.06
Eastern Block																
Jiao-Liao-Ji Belt	32.9	0.6	8.01	0.04	16.8	0.7	6.13	0.05	9.5	2.7	6.53	0.02	3.1	1.5	6.89	0.04
Huabei Plain	33.3	1.1	8.03	0.05	18.8	1.5	6.13	0.04	10.8	1.9	6.59	0.04	1.6	0.9	6.93	0.04
Yanshan Belt	33.4	1.6	8.07	0.04	22.4	1.1	6.14	0.03	8.9	2.4	6.57	0.05	2.4	0.5	6.88	0.03
Average	33.3	1.2	8.04	0.05	19.3	2.2	6.13	0.04	10.3	2.2	6.58	0.04	1.9	1.1	6.92	0.04
TNCO	37.2	2.4	8.02	0.05	21.6	1.4	6.13	0.04	12.5	1.0	6.60	0.05	2.0	0.9	6.93	0.04
Western Block																
Khondalite Belt	45.9	2.6	8.04	0.05	23.3	0.9	6.17	0.04	17.4	3.0	6.56	0.02	4.7	1.5	6.85	0.06
Ordos Basin	43.9	2.7	8.07	0.07	21.6	0.7	6.14	0.06	15.3	2.1	6.58	0.03	4.6	0.8	6.86	0.05
Yinshan Belt	45.8	3.5	8.02	0.04	24.7	1.2	6.13	0.04	17.5	3.5	6.54	0.02	4.4	1.7	6.88	0.07
Average	44.9	3.1	8.05	0.07	22.9	1.6	6.14	0.06	16.4	2.9	6.57	0.03	4.6	1.3	6.86	0.06
Orogen Belt																
Sulu Belt	31.5	1.0	7.99	0.06	16.6	0.4	6.16	0.06	11.8	1.9	6.54	0.04	1.6	0.8	6.93	0.09
Dabie-Qinling Belt	39.1	5.3	8.06	0.05	20.5	1.4	6.11	0.05	15.0	2.3	6.61	0.03	3.6	2.0	6.89	0.03
Qilian Belt	51.2	2.6	8.00	0.03	25.5	2.2	6.07	0.02	21.4	1.8	6.52	0.04	6.2	0.4	6.80	0.02

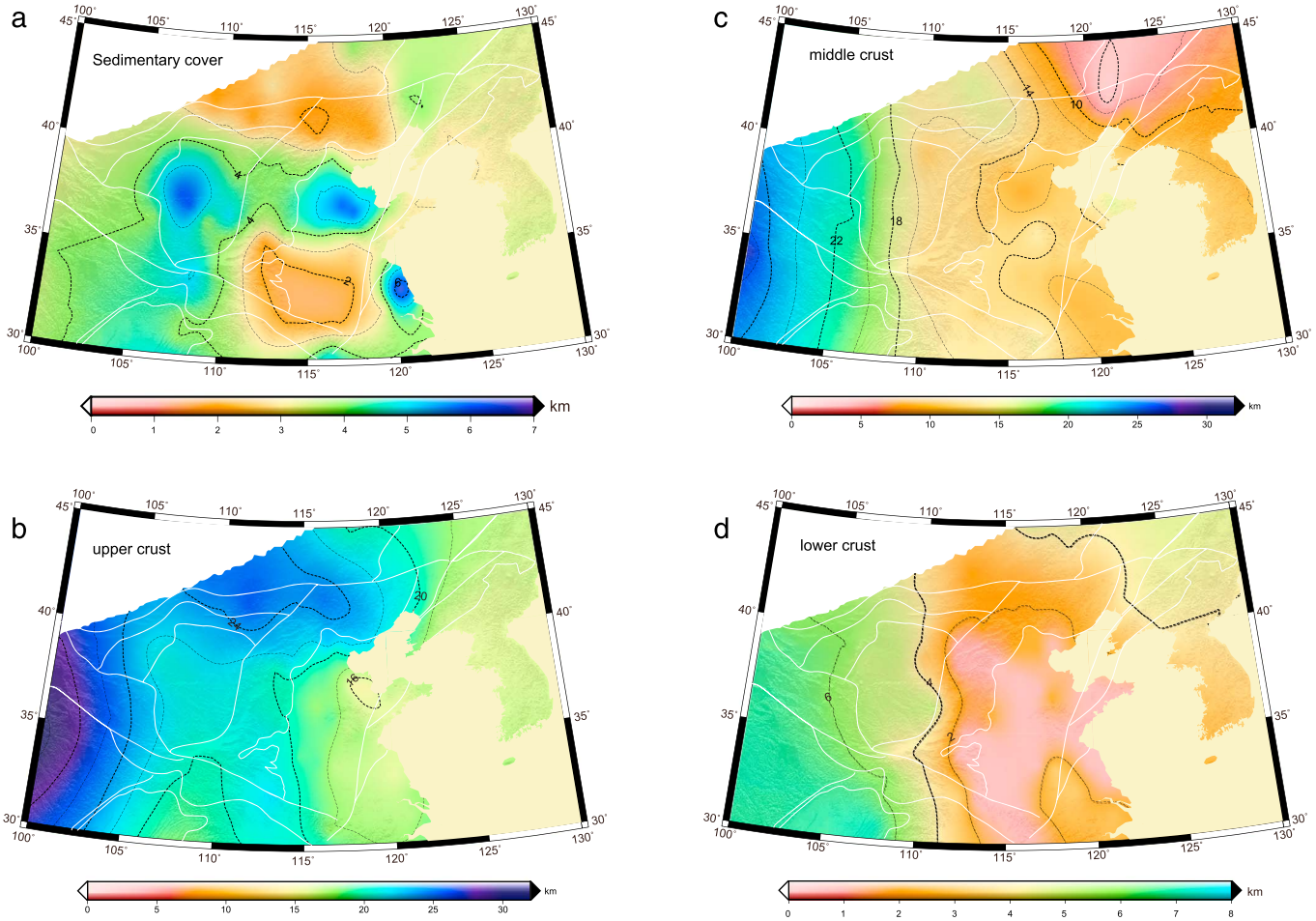

Figure 7. Thickness of the (a) sedimentary cover (V_p < 5.8 km/s), (b) upper crust (V_p = 5.8–6.4 km/s), (c) middle crust (V_p = 6.4–6.8 km/s), and (d) lower crust (V_p = 6.8–7.3 km/s).

However, despite of an overall similar pattern, the difference in the Moho depth between the NCcrust and the RF model is from −5 km to +5 km and locally it exceeds 10 km (Figure 5b), although one receiver function station in the northwestern part of the North China Craton shows a super thin crust with a 6 km difference. The largest discrepancy between the NCcrust and CRUST 1.0 of up to 8 km is in the southeastern part of the North China Craton (Figure 5a) and from −4 km to +4 km in most of the area. The difference between the NCcrust and the RF results is <2 km in most regions and up to 6 km in some parts of the Western Block (Figure 5b). The largest discrepancy is at the Ordos Basin and the Khondalite Belt, where the NCcrust model shows a deeper Moho (by 2–3 km) than the other models (Figures 6f and 6g). We note that for this region, the NCcrust is based on a significantly larger set of seismic data than the CRUST 1.0 model and RF results (Figures 1a and 5).

4.1.2. Internal Structure of the Crust

The sedimentary cover is, in general, 2–6 km thick. Thick sequences of sediments (5–6 km) are typical of the Ordos Basin and the northern part of the North China Plain. The northern part of the Sichuan Basin has a 4–5 km thick sedimentary sequence, similar to the Songliao Basin (3–4 km). The thickness of the sedimentary cover is smallest (only 2 km) in the southern part of the North China Plain in the northern part of the Trans-North China Orogen and in the Yanshan Belt.

Typical thicknesses of the upper crust, middle crust, and lower crust beneath the North China Craton are 16–24 km, 10–22 km, and 0–6 km, respectively (Table 3 and Figures 7 and 8).

1. All crustal layers show a systematic trend in thickness increase from the reworked Eastern Block, where the lowest values are observed along the coast, to the stable Western Block, where the largest values are

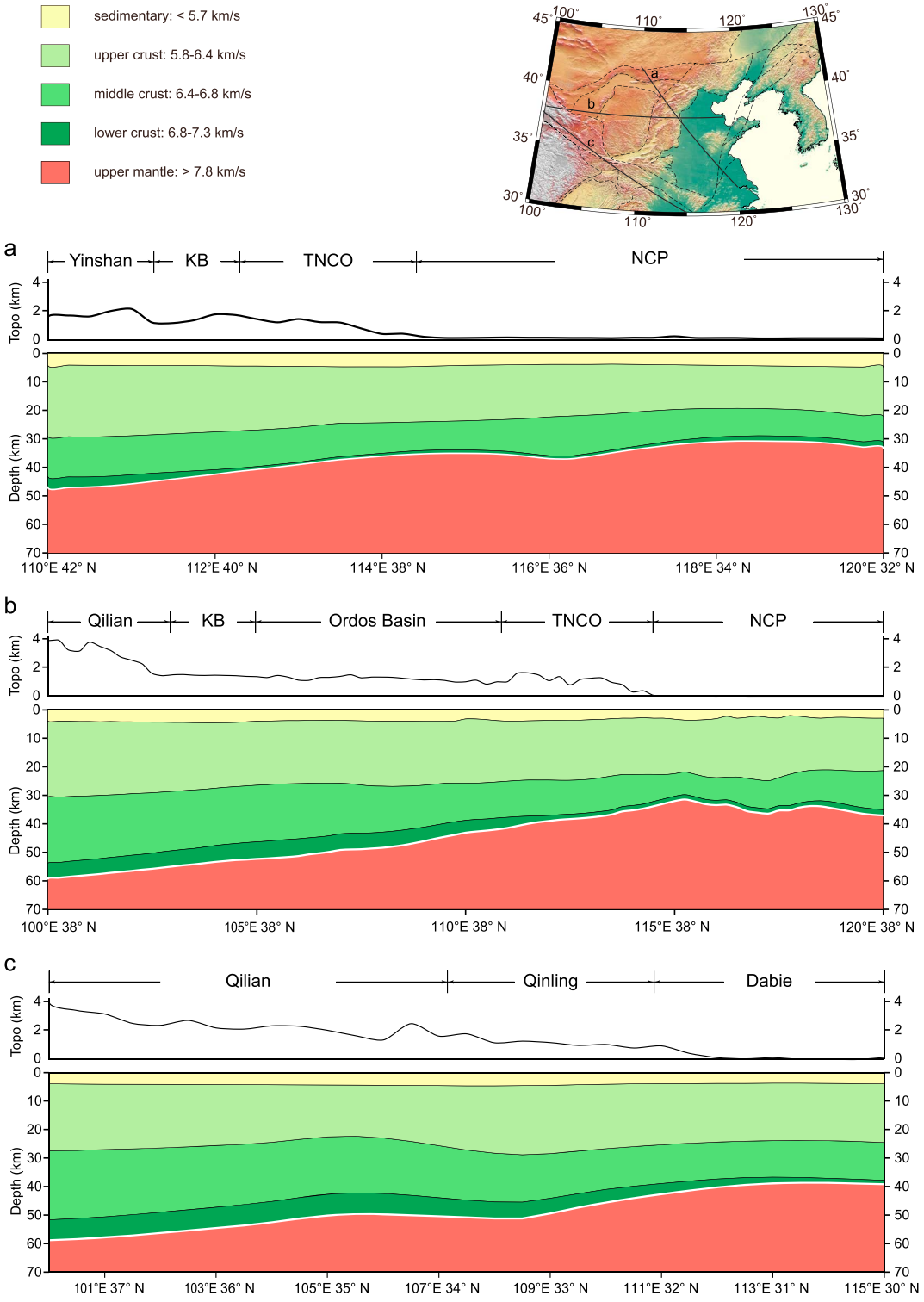

Figure 8. Crustal cross sections based on the new crustal model (Yinshan: the Yinshan Belt, KB: the Khondalite Belt, TNCO: the Trans-North China Orogen, NCP: the North China Plain).

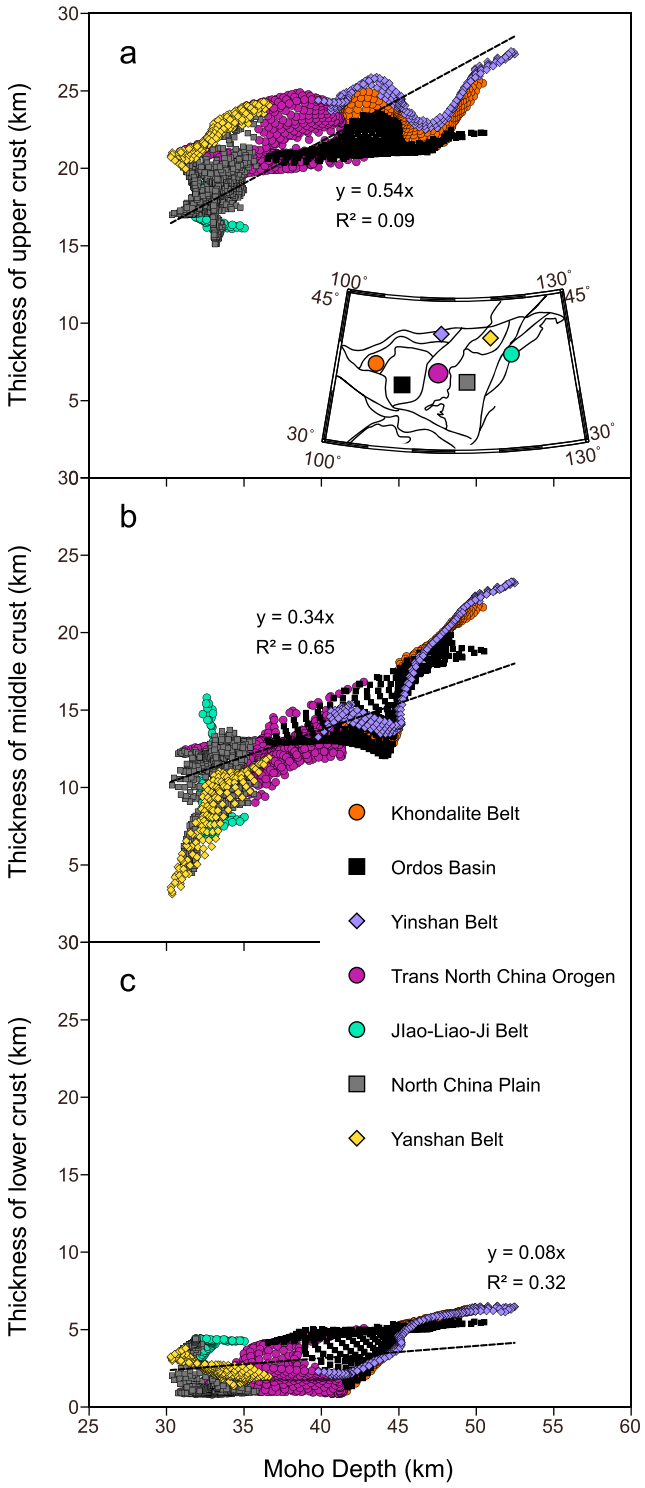

Figure 9. Moho depth versus thickness of (a) upper crust, (b) middle crust, and (c) lower crust in different provinces of the North China Craton.

observed (Figures 7 and 8). There is no correlation between the thickness of internal layers and tectonic blocks.

2. The upper crust of the whole North China Craton is relatively uniform in thickness which gradually increases from 16–20 km in the Eastern Block to 20–24 km in the Western Block. There is no clear correlation between the thickness of the upper crust and the Moho depth (Figure 9a)

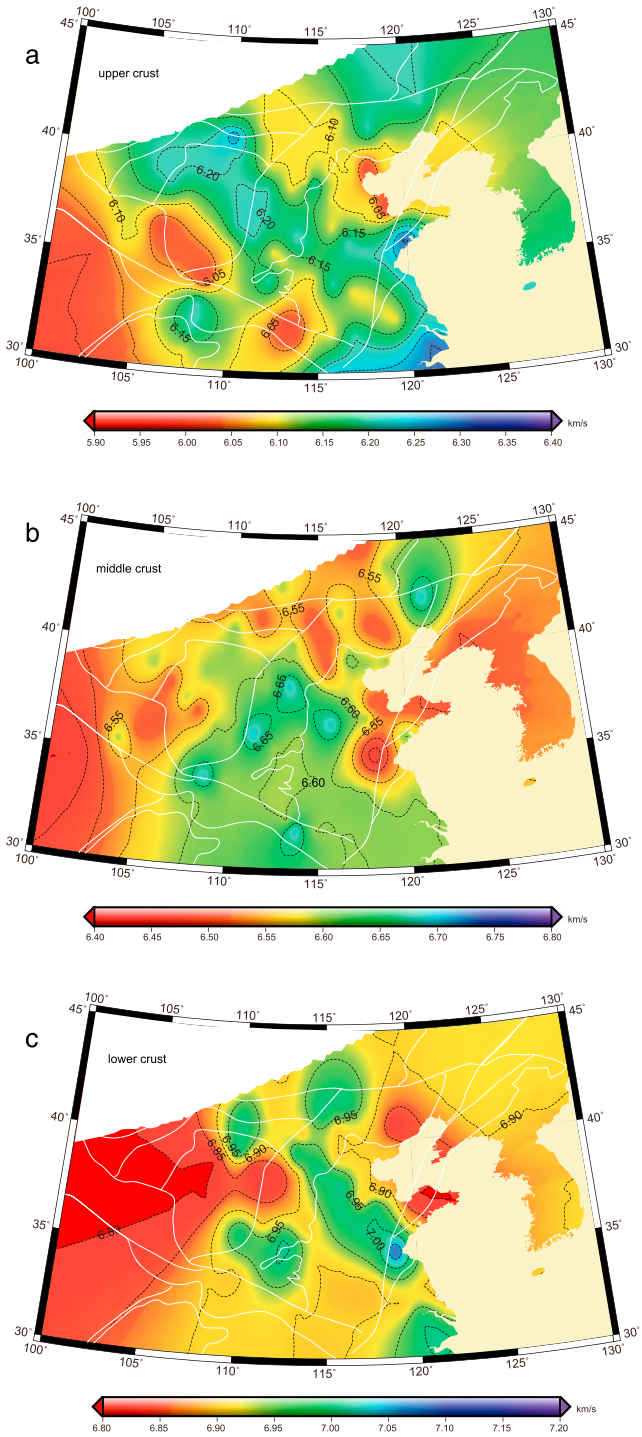

Figure 10. Average *P* wave velocity map of (a) upper crust (V_p = 5.8–6.4 km/s), (b) middle crust (V_p = 6.4–6.8 km/s), and (c) lower crust (V_p = 6.8–7.3 km/s).

3. The middle crust is 10–14 km thick in most part of the Eastern Block and up to 15–22 km thick in the Western Block with further increase to 26–28 km toward Tibet. The smallest thickness (<6 km) is typical of the Songliao Basin.
4. The thickness of the middle crust shows a strong correlation with the Moho depth for the whole North China Craton (Figure 9b), while the correlation between the thickness of the upper crust/lower crust and the Moho depth is relatively weak (Figures 9a and 9c). We therefore propose that it is chiefly heterogeneity

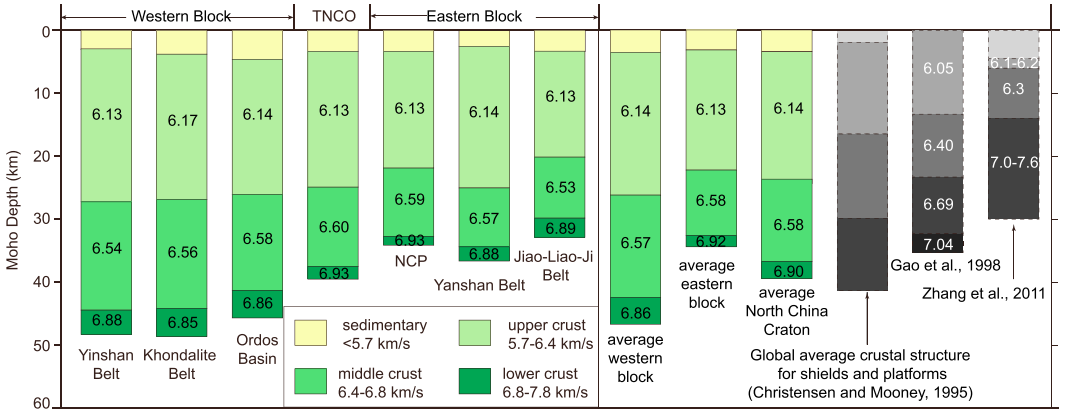

Figure 11. Crustal seismic velocity sections of different parts of the North China Craton, compared with the global average for continental crust [*Christensen and Mooney*, 1995] and previous models of the North China Craton [*Gao et al.*, 1998; *Zhang et al.*, 2011]. NCP: North China Plain, TNCO: Trans-North China Orogen.

of the middle crust that controls regional variations in Moho. This can be achieved through a viscous flow in a weak middle crustal layer, similar to observation for the East European Craton [*Artemieva*, 2007].

5. The lower crust in the North China Craton is 4–10 km thinner than the global average [*Christensen and Mooney*, 1995], and it is nearly absent in the tectonically reworked Eastern Block. This pattern is similar to the Phanerozoic Western Europe, where the lower crust is nearly absent as a result of the post-Variscan lithosphere delamination [*Artemieva and Meissner*, 2012].

While there is a systematic east-west trend in variations in the thickness of the crustal layers and the depth of Moho, there is no regular pattern in variations of the crustal V_p velocity neither in the individual crustal layers nor for the average crustal V_p. Crustal velocity heterogeneity also does not correlate with the tectonic boundaries between different crustal blocks (Figure 10).

The *P* wave velocity of the upper crust ranges from 6.05 km/s in the Ordos Basin and the northern part of the North China Plain to 6.10–6.15 km/s in most parts of the North China Plain and the Trans-North China Orogen to 6.20 km/s at the central and northern parts of the Western Block (Table 3 and Figures 10a and 11). Low *P* wave velocity (<6.55 km/s) is typical of the middle crust in the northern and eastern parts of the Eastern Block as well as in the southern part of the Ordos Basin. By the V_p velocities in the upper crust and middle crust, the Ordos Basin has two clear crustal blocks: northern with relatively high velocities and southern with relatively low velocities. This trend is, however, weakly matched in the variations in the thickness of the upper crust only.

The *P* wave velocity of the lower crust is <6.90 km/s in most parts of the Western Block and in particular beneath the Qilian Belt (Table 3 and Figures 10c and 11). We recognize a SE-NW trending belt of relatively high

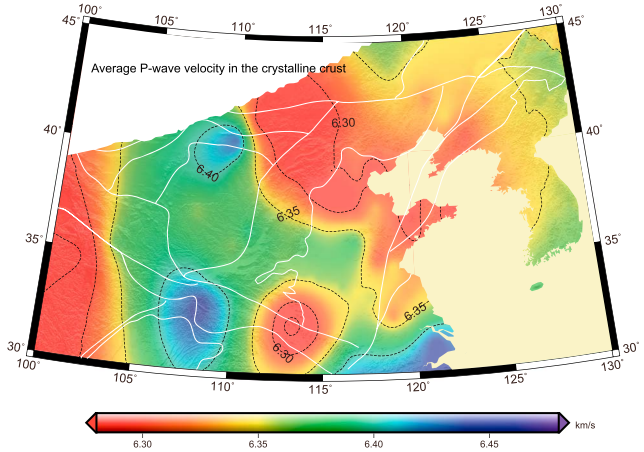

Figure 12. Average *P* wave velocity of the crystalline crust.

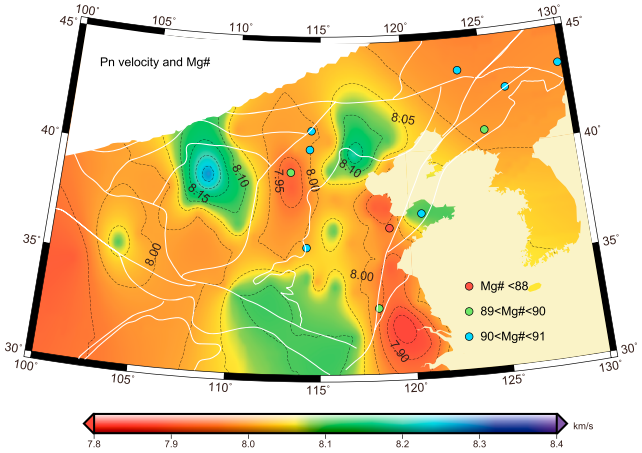

Figure 13. Map of *Pn* velocity. Colored dots: whole rock Mg# from Cenozoic mantle xenoliths (data from *Zheng et al*. [2007], and references therein).

lower crustal V_p (>6.95 km/s) across the central parts of the Trans-North China Orogen and the North China Plain, which apparently does not follow any known tectonic structures. It roughly corresponds to the SE-NW trending belt of relatively high upper crustal *P* wave velocities (>6.15 km/s).

On the whole, the average crustal V_p is low in the western and eastern parts and high in the central part of the NCC. The average *P* wave velocity in the crystalline crust ranges from 6.28 km/s in the northern part of the North China Plain, the northern part of the Trans-North China Orogen, and the Yinshan Belt, as well as in the central Qinling-Dabie Belt, to 6.42 km/s in the Khondalite Belt and the Ordos Basin with the highest values of ~6.45 km/s in the northwest Qinling-Dabie Belt (Table 3 and Figure 12).

4.1.3. *Pn* Velocity in the Uppermost Mantle

The worldwide average *Pn* velocity for shields and stable platforms is 8.1 ± 0.2 km/s [*Christensen and Mooney*, 1995]. The *Pn* velocity structure of the upper mantle beneath our study area is very heterogeneous with *Pn* values ranging from 7.8 km/s along the Tanlu Fault Zone to 8.3 km/s at the Ordos Basin (Figure 13). Regional variations in *Pn* velocities reflect variations both in lithosphere temperature and upper mantle composition. Geochemical studies of xenoliths suggest that the upper mantle is refractory with whole rock Mg# values of 90–91 (blue dots in Figure 9), which also suggest relatively low V_p values in the lithospheric mantle. Although some correlation is indicated between *Pn* velocity and Mg# (Figure 13), we do not observe any clear correlation between whole rock Mg# values (which are of pure compositional origin) and the upper mantle *Pn* velocities (which reflect variations in both composition and temperature) and therefore conclude that lateral variations in *Pn* velocity reflect primarily regional variations in lithosphere geotherms. With low heat flow, it is not a surprise that the *Pn* velocity in the Western Block is regionally up to 8.3 km/s (the northern part of the Ordos Basin). On the contrary, the Eastern block, which has experienced extensive reworking during the Mesozoic, has a high heat flow (~64 mW/m^2), a much thinner crust, and low *Pn* velocity, 8.0 km/s–8.1 km/s, with the lowest values of <7.9 km/s in the southern part of the North China Plain.

An extremely low *Pn* velocity (7.8–8.0 km/s), unusual for Archean cratons, is observed along the Tanlu Fault Zone. Mantle xenoliths from a depth of <60 km in Cenozoic basalts (16–2 Ma) within the translithospheric Tanlu Fault Zone have whole rock Mg# values of <90 (red and green dots in Figure 13) and suggest fertile mantle which may partly explain the low *Pn* velocity [*Xu et al*., 2000; *Zheng et al*., 1998, 2007]. Petrologic and geochemical data based on xenoliths in the Tanlu Fault Zone and the nearby area indicate that the lithospheric mantle is a mixture of the Archean-Proterozoic lithospheric mantle and Phanerozoic accreted material that has replaced the Archean lithospheric keel.

Similar to the Tanlu Fault Zone, the uppermost mantle of the northern and central parts of the Trans-North China Orogen is dominated by significantly low *Pn* velocities. These low *Pn* velocities are probably caused by the Late Mesozoic to Cenozoic basaltic magmatism [*Tang et al*., 2006]. *Pn* travel time tomography also identifies low upper mantle velocities beneath the Tanlu Fault Zone and the Trans-North China Orogen as well as a relatively high *Pn* velocity beneath the northern part of the Ordos Basin.

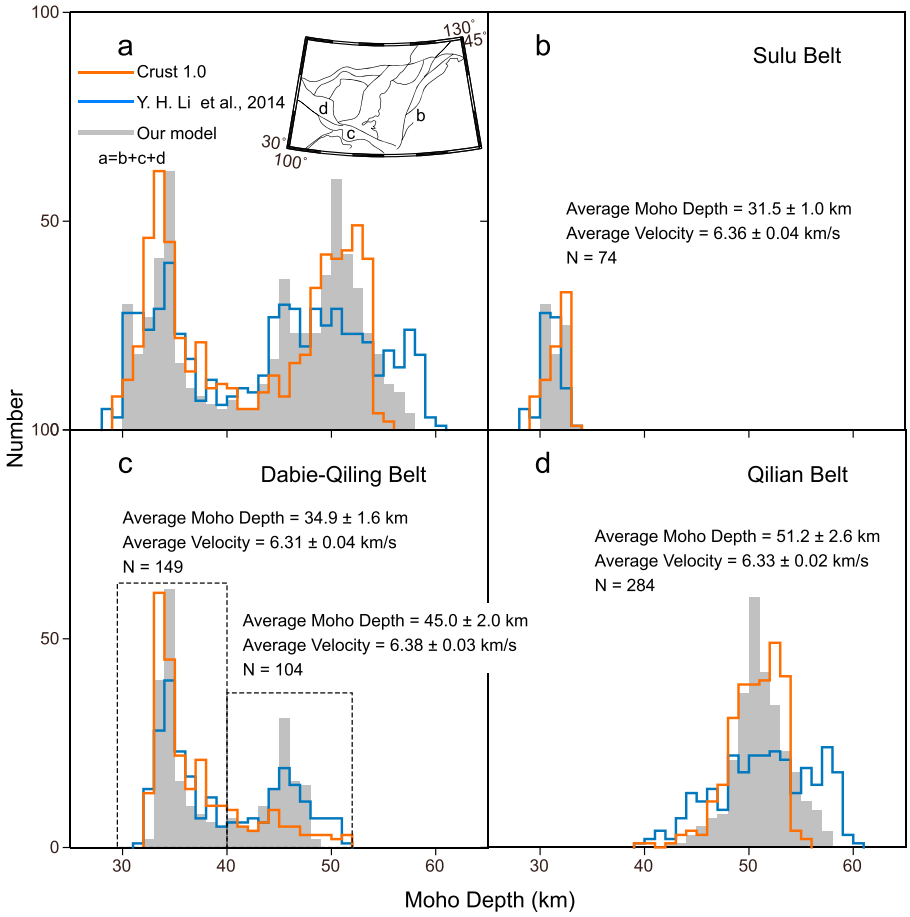

Figure 14. (a–d) Histogram of average Moho depth from different parts of the orogenic belts compared with the results from CRUST 1.0 and receiver function studies.

4.2. Surrounding Orogenic Belts

4.2.1. Moho Depth

We observe a strong difference in the structure of between the crust of the Sulu Belt in the east and the Dabie-Qinling and Qilian Belts in the west. According to geochemical studies, these Paleozoic-Early Mesozoic orogens contain diamond-bearing eclogite and coesite-bearing eclogite.

In the Sulu Belt the average crust is ~31 km thick and it is only slightly thicker (~36 km) in the Dabie Belt (Figures 3 and 14). These values are significantly smaller than global averages for the Cenozoic orogenic belts (Figure 15). We note that a similar crustal structure is typical of the Paleozoic Caledonides and Variscides in Europe [*Aichroth et al.*, 1992; *Artemieva and Thybo*, 2013] where the lower crust and the lithospheric mantle may have been delaminated [*Artemieva and Meissner*, 2012, and references therein] and of the Paleozoic Appalachians [*Tesauro et al.*, 2014, and references therein]. We therefore conclude that a thin crust beneath the Paleozoic-Early Mesozoic orogens of eastern China may be the result of lithosphere delamination caused by the Mesozoic Pacific subduction. However, because we cannot know the composition of the sub-Moho mantle, it is also possible that eclogite facies of crustal origin are present beneath the Moho.

The Dabie-Qinling orogen has a clearly different crustal structure beneath the Dabie Belt in the east and the Qinling Belt in the west. The difference in average crustal thickness amounts to ~10 km (Figure 14), with some difference in average crustal V_p. The Qinling orogen has an average Moho depth of 45 km which is larger than in the Phanerozoic orogens of Europe and North America.

Further to the west, the Qilian Belt at the northeastern margin of the Tibetan Plateau has a much thicker crust, up to 51 km on average, with regional variations between ~44 km and 58 km. Similarly, thick crust (down to

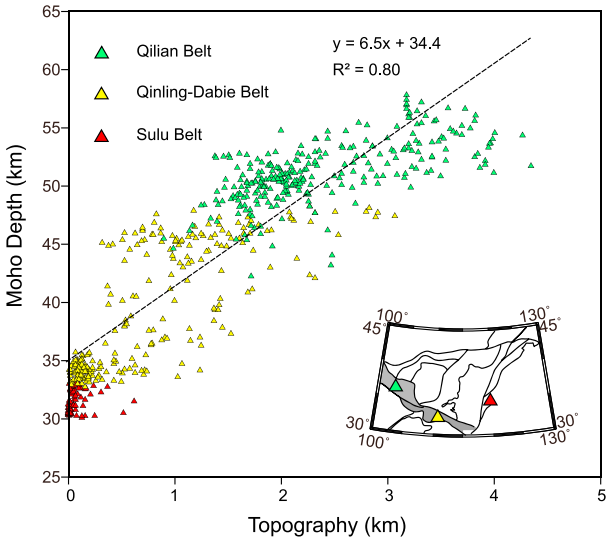

Figure 15. Topography versus Moho depth in the orogenic belts.

~60 km) is typical of the Paleozoic Uralides orogen preserved in the continental interior [*Artemieva and Thybo*, 2013, and references therein], but the mechanisms for making, and particularly for preserving, such thick crust may be different.

There is a strong linear correlation between the Moho depth and topography in all of the orogenic belts (Figure 15), which suggests a strong role of crustal Airy-type regional isostasy. This correlation is particularly strong for the Dabie-Qinling orogen which is close to isostatic equilibrium. We note that the slope of the correlation is different for the Dabie-Qinling (free-air gravity anomaly ~−20 mGal) and the Qilian Belts (free-air gravity anomaly range from −150 mGal to + 150 mGal), steep for the former and more gentle for the latter, indicating significant variation from regional isostasy in average crustal density along the orogenic belt. For the Sulu Belt the correlation between the Moho depth and topography is weak and indicates significant compositional heterogeneity of the crust.

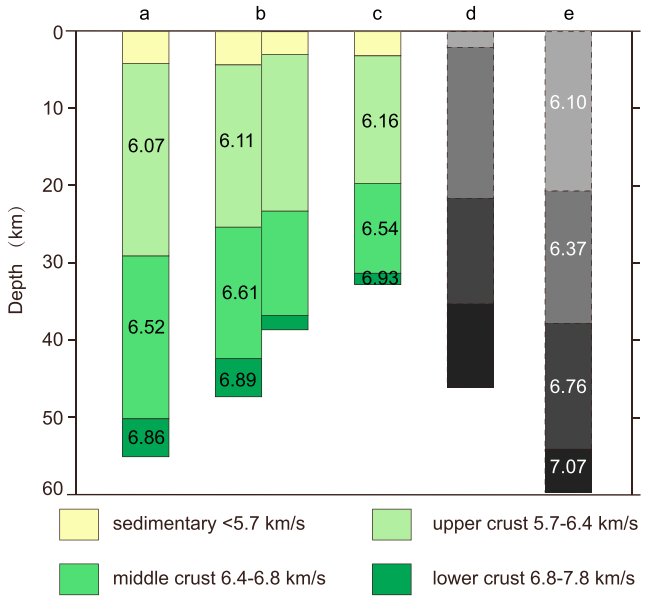

Figure 16. Crustal seismic velocity sections of the orogenic belts, compared with the global and regional averages for orogenic belts. (a) Qilian Belt, (b) Qinling-Dabie Belt, (c) Sulu Belt, (d) global average for orogenic belt [*Christensen and Mooney*, 1995], and (e) crustal structure model for Qinling from *Gao et al.* [1998].

4.2.2. Thickness of the Crustal Layers

The sedimentary cover is ~3–4 km thick in the entire orogenic belt. The thickness of the upper crust ranges from 15 km to 25 km in the Sulu-Dabie-Qinling Belt and from 20 km to nearly 30 km at Qilian. The upper crustal *P* wave velocity is low (<6.05 km/s) at the central Qilian Belt and the Qinling Belt (Figure 8a). The middle crust thickness varies between 10 km and 20 km at the Sulu-Dabie-Qinling Belt and between 16 km and 24 km at Qilian (Figures 7 and 16).

The Sulu Belt and the Qilian Belt have low *P* wave velocity (<6.55 km/s) in the middle crust (Figure 7b). The lower crust thickness ranges from nearly zero in the Sulu Belt and the Dabie Belt to ~5 km in the Qilian Belt and suggests lower crustal delamination or metamorphism. The V_p of the lower crust ranges from 6.80 km/s in the Qilian Belt and the northern Sulu Belt to 7.00 km/s in the central Sulu Belt (Figure 7c). The absence of a substantial high-velocity lower crustal layer suggests that there is no eclogite/garnet-granulite in the lower levels of the crust, but it does not exclude the presence in the uppermost mantle below the seismic Moho.

The correlation between Moho depth and thickness of the middle crust in the orogenic belt is relatively strong (Figure 17), while the upper crust and lower crust show weaker correlation in thickness with the Moho depth than the middle crust. This is similar to our observation for the North China craton in general. This observation may indicate that there has been reworking of both the upper crust and the lower crust, whereas the middle crust has been left relatively unaffected by these processes. Alternatively, middle crustal flow can be a major accommodation mechanism for the tectonic stresses.

5. Correlation Between the Moho Depth and Topography

Near-zero free-air gravity anomalies in the North China Craton indicate that this region is at almost complete isostatic equilibrium. Therefore, the topography is mostly controlled by lithosphere (crustal and mantle) thickness and density. A relatively strong correlation between Moho depth and topography (Figure 18a) suggests that the topography in the Western Block is mostly controlled by the crustal isostasy.

In the Eastern Block, we do not observe any correlation between the Moho depth and topography in the North China Plain (Figure 18b). As the region is isostatically compensated (free-air anomalies are 0 to ±20 mGal) we speculate that upper mantle heterogeneity and/or lateral density variations in the crust control the topography and the low topography may be caused by the presence of eclogitic crustal below the seismic Moho.

We observe a linear correlation between the topography and the Moho depth in the Trans-North China Orogen with a correlation coefficient of $R^2 = 0.44$ (Figure 18c). The free-air gravity anomaly ranges from −120 mGal to +120 mGal but the average is ~−20 mGal, suggesting an overall isostatic equilibrium in the Trans-North China Orogen, which should be essentially achieved through a combination of Airy-type compensation and variation in crustal and mantle density. However, the small slope, as for the eastern block, may suggest that other mechanism than crustal isostasy contributes to topography.

In the Western Block, the linear correlation between the topography and the Moho depth in the Ordos Basin is relatively strong with a correlation coefficient of $R^2 = 0.47$ (Figure 18d). Approximately ±30 mGal free-air gravity anomalies in the basin indicate that it is close to isostatic equilibrium. Our results demonstrate that Airy-type compensation plays an important role in regional isostasy (Figure 18d). In contrast to the orogens of the Eastern NCC, where the Moho depth and the topography are almost anticorrelated, no correlation is observed in the Khondalite and Yinshan orogens of the Western Block. We note that the Khondalite Belt and Yinshan Belt are not in isostatic equilibrium.

6. Geological Implications

The Archean crust of the NCC has undergone complex reworking by a large number of tectonothermal events, such as Paleozoic (~480 Ma) kimberlitic magmatic activity, Paleozoic (~440 Ma), and Early Mesozoic (~220 Ma) subduction and collision with the Yangtze block at its southern edge and Late Mesozoic (~135–115 Ma with a peak at ~120 Ma) widespread volcanism and intensive lithospheric extension.

Along the southeastern margin of the North China Craton with Moho depth <32 km, the discovery of eclogite xenoliths in the Mesozoic (~132 Ma) host rock of the NCC suggests that the crust beneath this area has been at least ~45 km thick in the Mesozoic [*Xu et al.*, 2006]. Presently, the crust is only 30–32 km thick along the

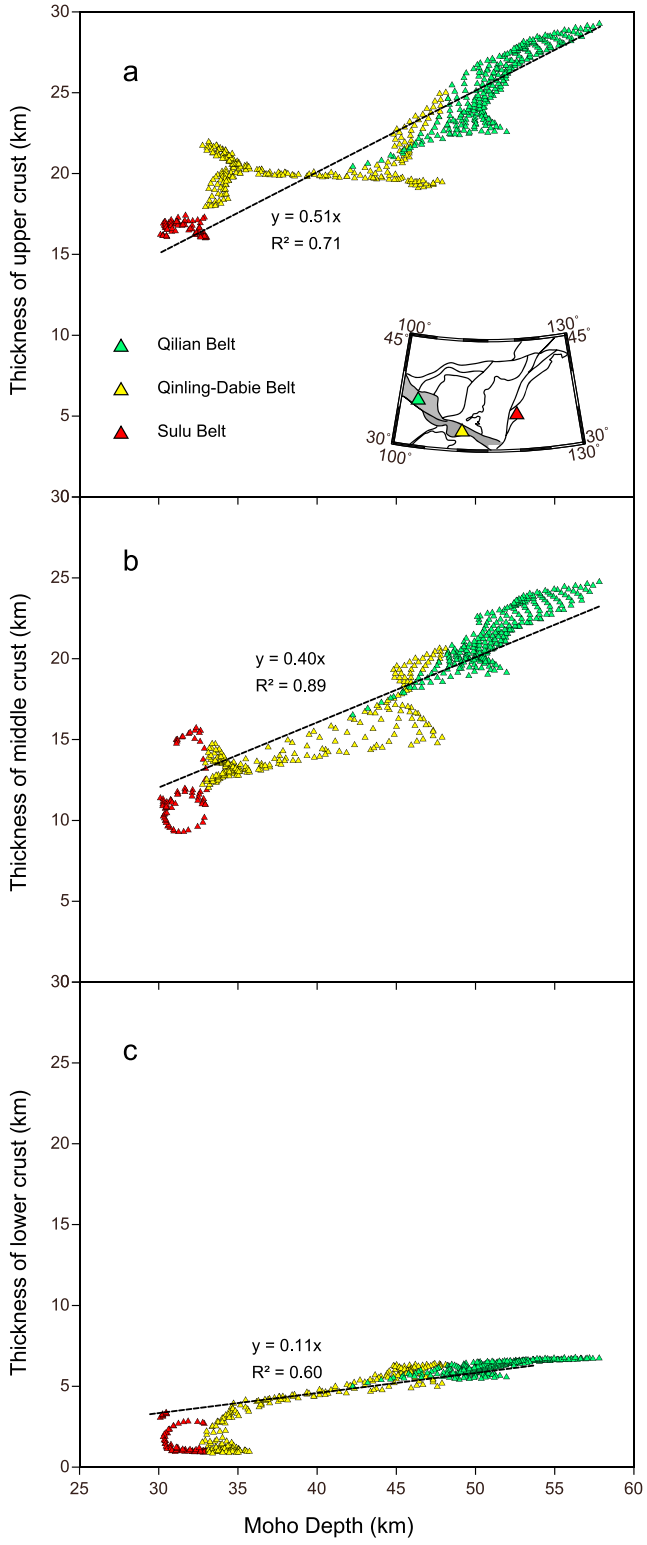

Figure 17. Moho depth versus thickness of (a) upper crust, (b) middle crust, and (c) lower crust in the orogenic belts.

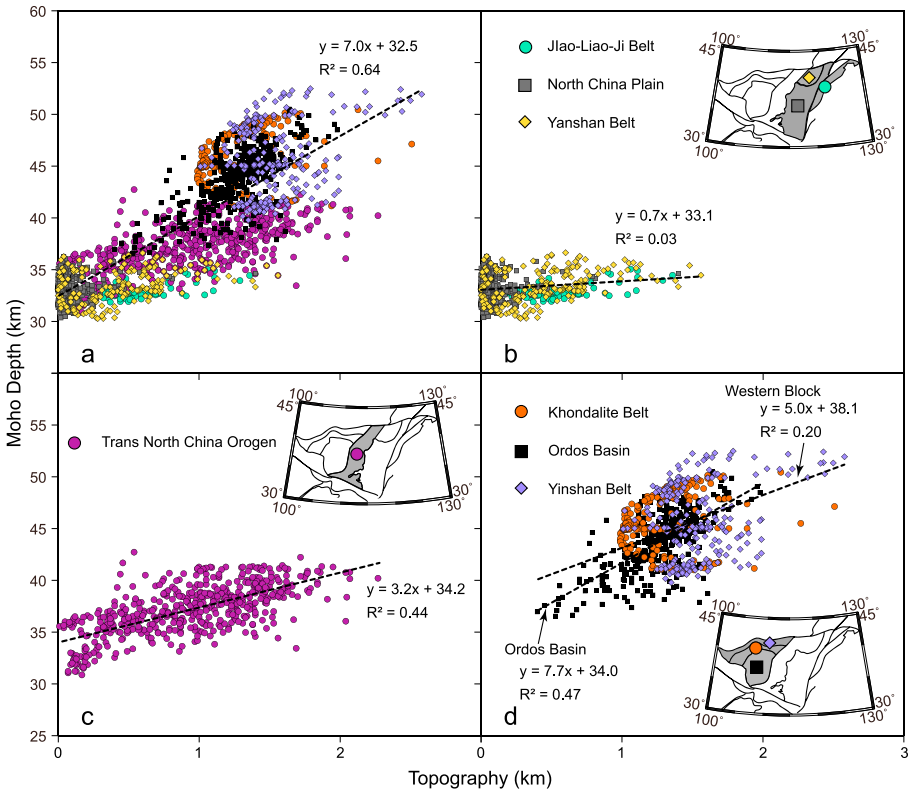

Figure 18. Topography versus Moho depth (a) for the North China Craton (NCC) as a whole and for its different tectonic provinces: (b) the Eastern Block of the NCC, (c) the TNCO of the North China Craton, and (d) the Western Block of the NCC. Small inserts with maps show locations of the tectonic provinces (gray shading and color symbols).

southeastern margin and has a sharp and flat Moho, similar to the Kaapvaal Craton [*Youssof et al.*, 2013] and Variscan Europe [*Artemieva and Meissner*, 2012]. Lower crustal xenoliths in the Cenozoic basalts from the surrounding areas consist of garnet-free granulite which is consistent with a Moho depth of ~30 km [*Huang et al.*, 2004] as indicated by seismic data. The shallow Moho together with the presence of high $Mg^{\#}$ diorite [*Liu et al.*, 2012; *Xu et al.*, 2006] indicate that delamination may be the cause of the thin crust or that the sub-Moho material to a depth of at least 45 km still consists of granulite in eclogite facies as has been proposed for Variscan Europe [*Mengel and Kern*, 1992]. The latter option may explain the presence of the deep sedimentary basin in this region as caused by isostatic subsidence due to formation of a high-density eclogitic crust.

In the northern part of the Eastern block, seismic data indicate a 30–36 km thick crust in the Yanshan Belt (Figure 3), but the presence of widespread Mesozoic adakitic rocks in this region has led to suggestions of thick (>50 km) crust during the Late Mesozoic (adakites require high-pressure partial melting) [*Zhang et al.*, 2008], which is consistent with the delamination model [*Gao et al.*, 2004] and with the presence of eclogites. However, the most recent trace-element modeling suggests that the melting depth of the Mesozoic adakitic rocks in the Yanshan Belt is between 33 km and 40 km [*Ma et al.*, 2015]. These values are consistent with the seismic data and the NCcrust model, which show that the average Moho depth in the Yanshan Belt is 32–35 km and therefore does not require that a thick Mesozoic crust should have been delaminated.

7. Conclusions

We present a new compilation of the crustal structure (NCcrust) of the North China Craton and the surrounding area based on all publicly available regional and local controlled-source seismic models and receiver function studies. Analysis of the crustal structure based on the NCcrust regional model shows the following:

1. There is a systematic increase in the total crustal thickness from east to west. We explain the presence of a thin (30–36 km) crust in the eastern North China Craton by tectonic processes related to the Mesozoic Pacific subduction, and lithosphere reworking and delamination, or possibly the presence of ecologite

facies crustal rocks below Moho. Our conclusion is supported by the absence of a lower crustal layer in this part of the North China Craton. In contrast, the crustal thickness up tp 52–56 km in the Western Block of the North China Craton, which is similar to the crustal thickness of the East European and Siberian cratons, may indicate the presence of preserved Archean crust.

2. The sedimentary cover in the NCC is 2–6 km thick. The deepest basins are the Ordos Basin and the northern part of the North China Plain (5–6 km). In the southern part of the North China Plain and in the northern part of the Trans-North China Orogen, the thickness of the sedimentary covers is only 2 km. There is a systematic westward increase in thicknesses of individual crustal layers. The thickness of the upper crust ranges from 10 km with *P* wave velocity of 6.05 km/s near the coast to 24 km with *P* wave velocity of 6.20 km/s in the Western Block. On average, the middle crust is ~10 km thick although it is up to 22 km thick in the Western Block with a relatively sharp east to west transition. The lower crust is almost absent (<2 km) in the Eastern Block as well as in the Trans-North China Craton, while in the Ordos Basin the lower crust is 6 km thick. We do not observe any correlation between the average crustal velocities and the crustal thickness. For individual crustal layers, the thickness of the middle crust is best correlated with the Moho depth, and we speculate that viscous flow in a rheological weak middle crust essentially controls regional variation in the crustal thickness.
3. The *Pn* velocity of the uppermost mantle is very heterogeneous with values ranging from 7.8 km/s to 8.2–8.4 km/s. Low *Pn* velocity (7.8 km/s) is observed along the Tanlu Fault Zone where it might indicate deep reaching faulting and in the northern-central part of the Trans-North China Orogen where it may be related to Mesozoic magmatic activity. High *Pn* velocity (8.3 km/s), typical of Archean cratons, is characteristic of the northern part of the Ordos Basin, whereas the southern part of the Ordos Basin has low *Pn* velocity (8.0 km/s).
4. The distribution of the crustal thickness in the Paleozoic-Mesozoic orogens at the southern and eastern margins of the NCC is clearly bimodal. Thin (30–35 km) crust is typical of the orogens in the east (the Sulu Belt and the Dabie Belt), while thick (45–58 km) crust is characteristic of the Qinling and Qilian Belts in the west. We attribute thin orogenic crust to crustal delamination related to the Mesozoic Pacific subduction, similar to the Paleozoic Variscan and Appalachian orogens. However, it is possible that the seismic Moho marks a phase change from mafic into eclogitic phases. We find that the crustal structure of the Sulu-Dabie Belt is similar to the Paleozoic European Caledonian and Appalachian orogens, while the thick crust of the Qilian Belt resembles the crust of the Paleozoic Ural Mountains. The UHP metamorphic belt is expressed by a relatively high velocity (8.1 km/s) *Pn* anomaly.
5. There is an overall linear correlation between the Moho depth and topography for almost the entire North China Craton ($R^2 = 0.64$). However, no correlation is found for individual tectonic provinces in the Khondalite and Yinshan orogens of the Western Block and the North China Plain of the Eastern Block. In contrast, a strong linear correlation between the topography and the Moho depth exists in the Trans-North China Orogen, and the Ordos Basin of the Western NCC, suggesting an important role of an Airy-type compensation in regional isostasy.

Acknowledgments

B.X. is supported by the National Science Foundation of China (91214204, 41130315, and 41520104003). I.A. acknowledges grant DFF-FNU-1323-00053 (Denmark), and H.T. acknowledges grant DFF-FNN-4002-00138 (Denmark). Special thanks go to Jiyan Lin for providing seismic data and original seismic publications. The data for this paper are available by contacting the corresponding authors.

References

Aichroth, B., C. Prodehl, and H. Thybo (1992), Crustal structure along the central segment of the EGT from seismic-refraction studies, *Tectonophysics 207*, *207*(1–2), 43–64, doi:10.1016/0040-1951(92)90471-H.

Angus, D. A., J. M. Kendall, D. C. Wilson, D. J. White, S. Sol, and C. J. Thomson (2009), Stratigraphy of the Archean western Superior Province from P- and S-wave receiver functions: Further evidence for tectonic accretion?, *Phys. Earth Planet. Inter.*, *177*(3–4), 206–216, doi:10.1016/j.pepi.2009.09.002.

Artemieva, I. M. (2007), Dynamic topography of the East European craton: Shedding light upon lithospheric structure, composition and mantle dynamics, *Global Planet. Change*, *58*(1–4), 411–434, doi:10.1016/j.gloplacha.2007.02.013.

Artemieva, I. M., and R. Meissner (2012), Crustal thickness controlled by plate tectonics: A review of crust-mantle interaction processes illustrated by European examples, *Tectonophysics*, *530–531*, 18–49, doi:10.1016/j.tecto.2011.12.037.

Artemieva, I. M., and H. Thybo (2013), EUNAseis: A seismic model for Moho and crustal structure in Europe, Greenland, and the North Atlantic region, *Tectonophysics*, *609*, 97–153, doi:10.1016/j.tecto.2013.08.004.

Bai, Z. M, and C. Y. Wang (2006), Crustal P-wave velocity structure in Lower Yangtze region: Reinterpretation of Fuliji-Fengxian deep seismic sounding profile, *Chin. Sci. Bull.*, *51*(9), 2391–2400, doi:10.1007/s11434-006-2115-z.

Cao, J. M, J. S. Zhu, and D. C. Wu (1994), Velocity Structure of the Crust in Eastern Qinling Mountain, *J. Chengdu Inst. Technol.*, *21*(1), 11–17.

Chen, L. (2012), Concordant structural variations from the surface to the base of the upper mantle in the North China Craton and its tectonic implications, *Lithos*, *120*(1–2), 96–115, doi:10.1016/j.lithos.2009.12.007.

Chen, L., C. Cheng, and Z. G. Wei (2009), Seismic evidence for significant lateral variations in lithospheric thickness beneath the central and western North China Craton, *Earth Planet. Sci. Lett.*, *286*(1–2), 171–183, doi:10.1016/j.epsl.2009.06.022.

Chen, L., M. M. Jiang, J. H. Yang, Z. G. Wei, C. Z. Liu, and Y. Ling (2014), Presence of an intralithospheric discontinuity in the central and western North China Craton: Implications for destruction of the craton, *Geology*, *42*(3), 223–226, doi:10.1130/g35010.1.

Cheng, C., L. Chen, H. J. Yao, M. M. Jiang, and B. Y. Wang (2013), Distinct variations of crustal shear wave velocity structure and radial anisotropy beneath the North China Craton and tectonic implications, *Gondwana Res.*, *23*(1), 25–38, doi:10.1016/j.gr.2012.02.014.
Cherepanova, Y., I. M. Artemieva, H. Thybo, and Z. Chemia (2013), Crustal structure of the Siberian craton and the West Siberian basin: An appraisal of existing seismic data, *Tectonophysics*, *609*, 154–183, doi:10.1016/j.tecto.2013.05.004.
Chinese State Seismological Bureau (CSSB) (1988), *Lithosphere and Dynamics Atlas of China*, China Cartographic Publishing House, Beijing.
Chinese State Seismological Bureau (CSSB), Deep Exploration Group (DEG) (1986), *Results of Geophysical Investigation in China, Crust and Upper Mantle. (in Chinese)*, China Seismological Press, Beijing.
Chinese State Seismological Bureau (CSSB) (1995), *United Observing Group of Triangle Explosion*, pp. 140–153, Geological Publishing House, Beijing.
Cho, H. M., C. E. Baag, J. M. Lee, W. M. Moon, H. Jung, K. Y. Kim, and I. Asudeh (2006), Crustal velocity structure across the southern Korean Peninsula from seismic refraction survey, *Geophys. Res. Lett.*, *33*, L06307, doi:10.1029/2005GL025145.
Cho, H. M., C. E. Baag, J. M. Lee, W. M. Moon, H. Jung, and K. Y. Kim (2013), P- and S-wave velocity model along crustal scale refraction and wide-angle reflection profile in the southern Korean peninsula, *Tectonophysics*, *582*, 84–100, doi:10.1016/j.tecto.2012.09.025.
Christensen, N. I., and W. D. Mooney (1995), Seismic velocity structure and composition of the continental crust: A global view, *J. Geophys. Res.*, *100*(B6), 9761–9788, doi:10.1029/95JB00259.
Cook, F. A., D. J. White, A. G. Jones, D. W. S. Eaton, J. Hall, and R. M. Clowes (2010), How the crust meets the mantle: Lithoprobe perspectives on the Mohorovičić- discontinuity and crust-mantle transition, *Can. J. Earth Sci.*, *47*, 315–351, doi:10.1139/E09-076.
Ding, Y. Y, J. M. Cao, C. J. Huang, and G. F. Jiang (1987), A preliminary study of the structure of the Earth's crust for the profile from Suixian to Xian, *Acta Geophys. Sin.*, *30*(1), 31–38.
Dong, S. W., X. Z. Wu, R. Gao, D. Y. Lu, Y. K. Li, Y. Q. He, J. F. Tang, F. Y. Cao, M. J. Hou, and D. Z. Huang (1998), On the crust velocity levels and dynamics of the Dabieshan orogenic belt, *Acta Geophys. Sin.*, *41*(3), 349–361.
Duan, Y. H., B. J. Liu, J. R. Zhao, B. F. Liu, C. K. Zhang, S. Z. Pan, J. Y. Lin, and W. B. Guo (2015), 2-D P-wave velocity structure of lithosphere in the North China tectonic zone: Constraints from the Yancheng-Baotou deep seismic profile, *Sci. China Earth Sci.*, *58*(9), 1577–1591, doi:10.1007/s11430-015-5081-y.
Duan, Y. H., F. Y. Wang, X. K. Zhang, J. Y. Lin, Z. Liu, B. F. Liu, Z. X. Yang, W. B. Guo, and Y. B. Wei (2016), Three-dimensional crustal velocity structure model of the middle-eastern north China Craton (HBCrust1.0), *Sci. China Earth Sci.*, *59*(7), 1477–1488, doi:10.1007/s11430-016-5301-0.
Durrheim, R. J., and R. W. Green (1992), A seismic refraction investigation of the Archean Kaapvaal Craton, South Africa, using mine tremors as the energy source, *Geophys. J. Int.*, *108*(3), 812–832, doi:10.1111/j.1365-246x.1992.tb03472.x.
Frassetto, A., and H. Thybo (2013), Receiver function analysis of the crust and upper mantle in Fennoscandia—Isostatic implications, *Earth Planet. Sci. Lett.*, *381*, 234–246, doi:10.1016/j.epsl.2013.07.001.
Gao, S., B. R. Zhang, Z. M. Jin, H. Kern, T. C. Luo, and Z. D. Zhao (1998), How mafic is the lower continental crust?, *Earth Planet. Sci. Lett.*, *161*(1–4), 101–117, doi:10.1016/S0012-821X(98)00140-X.
Gao, S., H. Kern, Y.-S. Liu, S.-Y. Jin, T. Popp, Z.-M. Jin, J.-L. Feng, M. Sun, and Z.-B. Zhao (2000), Measured and calculated seismic velocities and densities for granulites from xenolith occurrences and adjacent exposed lower crustal sections: A comparative study from the North China craton, *J. Geophys. Res.*, *105*(B8), 18,965–18,976, doi:10.1029/2000JB900100.
Gao, S., R. L. Rudnick, H. L. Yuan, X. M. Liu, Y. S. Liu, W. L. Xu, W. L. Ling, J. Ayers, X. C. Wang, and Q. H. Wang (2004), Recycling lower continental crust in the North China craton, *Nature*, *432*(7019), 892–897, doi:10.1038/nature03162.
Geng, Y. S, L. L. Du, and L. Ren (2012), Growth and reworking of the early Precambrian continental crust in the North China Craton: Constraints from zircon Hf isotopes, *Gondwana Res.*, *21*(23), 517–529, doi:10.1016/j.gr.2011.07.006.
Guo, L. H., X. H. Meng, L. Shi, and Z. X. Chen (2012), Preferential filtering method and its application to Bouguer gravity anomaly of Chinese continent, *Chin. J. Geophys.*, *55*(12), 4078–4088, doi:10.6038/j.issn.0001-5733.2012.12.020.
He, L. J. (2015), Thermal regime of the North China Craton: Implications for craton destruction, *Earth Sci. Rev.*, *140*, 14–26, doi:10.1016/j.earscirev.2014.10.011.
He, R. Z, X. F. Shang, C. Q. Yu, H. J. Zhang, and R. D. Van der Hilst (2014), A unified map of Moho depth and Vp/Vs ratio of continental China by receiver function analysis, *Geophys. J. Int.*, *199*(3), 1910–1918, doi:10.1093/gji/ggu365.
Herceg, M., I. M. Artemieva, and H. Thybo (2016), Sensitivity analysis of crustal correction for calculation of lithospheric mantle density from gravity data, *Geophys. J. Int.*, *204*(2), 687–696, doi:10.1093/gji/ggv431.
Hu, H. X., X. B. Chen, B. X. Zhang, W. R. Song, Z. H. Xiao, and Z. Q. He (1986), On the interpretation of the DSS data of Suixian-Anyang Profile in central China, *Acta Seismol. Sin.*, *8*(1), 37–49.
Huang, X. L., Y. G. Xu, and D. Y. Liu (2004), Geochronology, petrology and geochemistry of the granulite xenoliths from Nushan, east China: Implication for a heterogeneous lower crust beneath the Sino-Korean Craton, *Geochim. Cosmochim. Acta*, *68*(1), 127–149, doi:10.1016/S0016-7037(03)00416-2.
Jia, S. X., and C. Q. Liu (1991), Interpretation of Heze-Changzhi DSS profile in south of the basin in North China, *North China Earthquake Sci.*, *9*(2), 11–20.
Jia, S. X., and C. Q. Liu (1991), Interpretation of Heze-Changzhi DSS profile in south of the basin in North China, *North China Earthquake Sci.*, *9*(2), 11–20.
Jia, S. X., F. Y. Wang, X. F. Tian, Y. H. Duan, J. S. Zhang, B. F. Liu, and J. Y. Lin (2014), Crustal structure and tectonic study of North China Craton from a long deep seismic sounding profile, *Tectonophysics*, *627*, 48–56, doi:10.1016/j.tecto.2014.04.013.
Kaban, M. K., P. Schwintzer, I. M. Artemieva, and W. D. Mooney (2003), Density of the continental roots: Compositional and thermal contributions, *Earth Planet. Sci. Lett.*, *209*(1–2), 53–69, doi:10.1016/s0012-821x(03)00072-4.
Lai, X. L., X. K. Zhang, S. X. Cheng, and S. M. Fang (2004), Study on crust-mantle transitional zone in west margin of Zhangjiakou-Bohai fault belt, *Chin. J. Geophys.*, *47*(5), 798–804, doi:10.1002/cjg2.567.
Laske, G., G. Masters, Z. Ma, and M. Pasyanos (2013), *Update on CRUST1. 0-A 1-Degree Global Model of Earth's crust*, EGU General Assembly Conference Abstracts, Vienna, Austria.
Li, Q. L., F. Y. Wu, X. H. Li, Z. L. Qiu, Y. Liu, Y. H. Yang and G. Q. Tang (2011), Precisely dating Paleozoic kimberlites in the North China Craton and Hf isotopic constrains on the evolution of the subcontinental lithospheric mantle, *Lithos*, *126*(1-2), 127–134, doi:10.1016/j.lithos.2011.07.001.
Li, S. G., et al. (1993), Collision of the North China and Yangtse Blocks and formation of coesite-bearing eclogites: Timing and processes, *Chem. Geol.*, *109*(1), 89–111, doi:10.1016/0009-2541(93)90063-O.
Li, S. L, X. L. Lai, B. F. Liu, Z. S. Wang, J. Y. He, and Y. Sun (2011), Differences in lithospheric structures between two sides of Taihang Mountain obtained from the Zhucheng-Yichuan deep seismic sounding profile, *Sci. China Earth Sci.*, *54*(6), 871–880, doi:10.1007/s11430-011-4191-4.

Li, S. G., et al. (1993), Collision of the North China and Yangtse Blocks and formation of coesite-bearing eclogites: Timing and processes, *Chem. Geol.*, *109*(1), 89–111, doi:10.1016/0009-2541(93)90063-O.
Li, S. L., and W. D. Mooney (1998), Crustal structure of China from deep seismic sounding profiles, *Tectonophysics*, *288*(14), 105–113, doi:10.1016/S0040-1951(97)00287-4.
Li, S. L., W. D. Mooney, and J. C. Fan (2006), Crustal structure of mainland China from deep seismic sounding data, *Tectonophysics*, *420*(1–2), 239–252, doi:10.1016/j.tecto.2006.01.026.
Li, S. L., X. K. Zhang, C. K. Zhang, J. R. Zhao, and S. X. Cheng (2002), A preliminary study on the crustal velocity structure of Maqin-Lanzhou-Jingbian by means of deep seismic sounding profile, *Chin. J. Geophys.*, *45*(2), 209–216, doi:10.1002/cjg2.233.
Li, W. H. (2013), Joint exploration of deep deismic reflection and deep seismic sounding with its application in crust structure research, dissertation submitted to Chinese Academy of Gological Sciences For Doctor Degree, pp. 117–139.
Li, W. H., R. Gao, G. R. Kaller, Q. S. Li, H. S. Hou, Y. K. Li, and S. H. Zhang (2014), Crustal structure of the northern margin of the North China Craton from Huailai to Sonid Youqi profile, *Chin. J. Geophys.*, *57*(2), 472–483, doi:10.6038/cjg20140213.
Li, Y. H., M. T Gao, and Q. G Wu (2014), Crustal thickness map of the Chinese mainland from teleseismic receiver functions, *Tectonophysics*, *611*, 51–60, doi:10.1016/j.tecto.2013.11.019.
Liu, C. Q., S. X. Jia, and G. H. Du (1991), Result of seismic refraction sounding along the transect from Xiangshui, Jiangsu, to Mondula, Neimongol, *Seismolog. Geol.*, *13*(3), 193–204.
Liu, D. Y., A. P. Nutman, W. Compston, J. S. Wu, and Q. H. Shen (1992), Remnants of ≥3800 Ma crust in the Chinese part of the Sino-Korean craton, *Geology*, *20*(4), 339–342, doi:10.1130/0091-7613(1992)020<0339:ROMCIT>2.3.CO;2.
Liu, S. S., S. G. Li, S. S. Guo, Z. H. Hou, and Y. S. He (2012), The Cretaceous adakitic-basaltic-granitic magma sequence on south-eastern margin of the North China Craton: Implications for lithospheric thinning mechanism, *Lithos*, *134*, 163–178, doi:10.1016/j.lithos.2011.12.015.
Lu, Z. X., and H. K. Xia (1993), Geoscience transect from Dong Ujimqinqi, Nei Mongol, to Donggou, Liaoning, China, *Acta Geophys. Sin.*, *36*(6), 765–772.
Ma, Q., J. P. Zheng, Y. G. Xu, W. L. Griffin, and R. S. Zhang (2015), Are continental "adakites" derived from thickened or foundered lower crust?, *Earth Planet. Sci. Lett.*, *419*, 125–133, doi:10.1016/j.epsl.2015.02.036.
Mengel, K., and H. Kern (1992), Evolution of the petrological and seismic Moho-implications for the continental crust-mantle boundary, *Terra Nova*, *4*(1), 109–116, doi:10.1111/j.1365-3121.1992.tb00455.x.
Mooney, W. D., G. Laske, and T. G. Masters (1998), CRUST 5.1: A global crustal model at 5° × 5°, *J. Geophys. Res.*, *103*(B1), 727–747, doi:10.1029/97JB02122.
Nie, W. Y, Z. P. Zhu, X. K. Zhang, C. K. Zhang, Y. J. Gai, and J. S. Zhang (1998), The crustal-mantle tectonics and its velocity structure recealed by the refraction profile passing through the west edge of the Zhangjiakou-Bohai seismic belt, *J. Seismol. Res.*, *21*(1), 94–102.
Niu, F., and D. E. James (2002), Fine structure of the lowermost crust beneath the Kaapvaal Craton and its implications for crustal formation and evolution, *Earth Planet. Sci. Lett.*, *200*(1–2), 121–130, doi:10.1016/S0012-821X(02)00584-8.
Ren, Q. F., C. K. Zhang, J. R. Zhao, X. K. Zhang, and Z. P. Zhu (1992), Characteristics of crystal structures in Heze Region and earthquakes, *North China Earthquake Sci.*, *10*(3), 45–52.
Song, B., A. P. Nutman, D. Liu, and J. Wu (1996), 3800 to 2500 Ma crustal evolution in the Anshan area of Liaoning Province, northeastern China, *Precambrian Res.*, *78*(13), 79–94, doi:10.1016/0301-9268(95)00070-4.
Song, S. G., Y. L. Niu, L. Su, and X. H. Xia (2013), Tectonics of the North Qilian orogen, NW China, *Gondwana Res.*, *23*(4), 1378–1401, doi:10.1016/j.gr.2012.02.004.
Stolk, W., M. Kaban, F. Beekman, M. Tesauro, W. D. Mooney, and S. Cloetingh (2013), High resolution regional crustal models from irregularly distributed data: Application to Asia and adjacent areas, *Tectonophysics*, *602*, 55–68, doi:10.1016/j.tecto.2013.01.022.
Stratford, W., and H. Thybo (2011), Seismic structure and composition of the crust beneath the southern Scandes, Norway, *Tectonophysics*, *502*, 364–382, doi:10.1016/j.tecto.2011.02.008.
Sun, S. S., S. C. Ji, Q. Wang, M. Salisbury, and H. Kern (2012), P-wave velocity differences between surface-derived and core samples from the Sulu ultrahigh-pressure terrane: Implications for in situ velocities at great depths, *Geology*, *40*(7), 651–654, doi:10.1130/g33045.1.
Sun, W. C., S. L. Li, and C. C. Yang (1985), Pleminary study on crustal structures in the east of north China, *Seismol. Geol.*, *7*(3), 1–12.
Sun, Y. S., X. Li, S. Kuleli, F. Dale Morgan, and M. N. Toksoz (2004), Adaptive moving window method for 3D P-velocity tomography and its application in China, *Bull. Seismol. Soc. Am.*, *94*(2), 740–746, doi:10.1785/0120030129.
Sun, Y. S., M. N. Toksoz, S. Pei, and F. D. Morgan (2008), The layered shear-wave velocity structure of the crust and uppermost mantle in China, *Bull. Seismol. Soc. Am.*, *98*(2), 746–755, doi:10.1785/0120050222.
Tang, Y. J., H. F. Zhang, and J. F. Ying (2006), Asthenosphere-lithospheric mantle interaction in an extensional regime: Implication from the geochemistry of Cenozoic basalts from Taihang Mountains, North China Craton, *Chem. Geol*, *233*(34), 309–327, doi:10.1016/j.chemgeo.2006.03.013.
Teng, J. W. (1985), Explosion seismological study for velocity distribution and structure of the crust and upper mantle from Maanshan to Qidong of the Southern parts of China, *Acta Geophys. Sin.*, *28*(2), 155–169.
Teng, J. W., et al. (2010), Velocity distribution of upper crust, undulation of sedimentary formation and crystalline basement beneath the Ordos Basin in North China, *Chin. J. Geophys.*, *52*(1), 277–291, doi:10.1002/cjg2.1348.
Teng, J. W., Z. J. Zhang, X. K. Zhang, C. Y. Wang, R. Gao, B. J. Yang, Y. H. Qiao, and Y. F. Deng (2013), Investigation of the Moho discontinuity beneath the Chinese mainland using deep seismic sounding profiles, *Tectonophysics*, *609*, 202–216, doi:10.1016/j.tecto.2012.11.024.
Tesauro, M., M. K. Kaban, W. D. Mooney, and S. Cloetingh (2014), NACr14: A 3D model for the crustal structure of the North American Continent, *Tectonophysics*, *631*(0), 65–86, doi:10.1016/j.tecto.2014.04.016.
Teng, J. W., S. L. Li, Y. Q. Zhang, F. Y. Wang, J. L. Pi, J. R. Zhao, C. K. Zhang, Y. H. Qiao, G. Z. Hu, and Y. F. Yan (2014), Fine velocity structures and deep processes in crust and mantle of the Qinling orogenic belt and the adjacent North China craton and Yangtze craton, *Chin. J. Geophys.*, *57*(10), 3154–3175, doi:10.6038/cjg20141006.
Tian, X. B, C. A. Zelt, F. Y. Wang, S. X. Jia, and Q. X. Liu (2014), Crust structure of the North China Craton from a long-range seismic wide-angle-reflection/refraction data, *Tectonophysics*, *634*, 237–245, doi:10.1016/j.tecto.2014.07.008.
Tseng, C. Y., H. J. Yang, H. Y. Yang, D. Liu, C. Wu, C. K. Cheng, C. H. Chen, and C. M. Ker (2009), Continuity of the North Qilian and North Qinling orogenic belts, Central Orogenic System of China: Evidence from newly discovered Paleozoic adakitic rocks, *Gondwana Res.*, *16*(2), 285–293, doi:10.1016/j.gr.2009.04.003.
Wang, C. Y, Z. F. Ding, J. L. Song, Q. G. Wu, J. Z. Zheng, and X. B. Zhang (1997), Shear wave velocity structure in Dabieshan orogenic belt, *Acta Geophys. Sin.*, *40*(3), 337–346.
Wang, C. Y., Z. Qi, Q. Qing, and M. F. Zho (2005), Geochemistry of the Early Paleozoic Baiyin volcanic rocks (NW China): Implications for the tectonic evolution of the North Qilian orogenic belt, *J. Geol.*, *113*(1), 83–94, doi:10.1086/425970.

Wang, C. Y., E. Sandvol, L. P. Zhu, H. Lou, Z. X. Yao, and X. H. Luo (2014), Lateral variation of crustal structure in the Ordos block and surrounding regions, North China, and its tectonic implications, *Earth Planet. Sci. Lett.*, *387*, 198–211, doi:10.1016/j.epsl.2013.11.033.

Wang, F. Y., X. K. Zhang, Y. Chen, L. Li, Q. F. Chen, J. R. Zhao, J. S. Zhang, and B. F. Liu (2004), 2-D P-wave velocity structure in the mideast segment of Zhangjiakou-Bohai tectonic zone: Anxin-Xianghe-Kuancheng DSS profile, *Acta Seismol. Sin.*, *17*, 31–41, doi:10.1007/s11589-004-0064-7.

Wang, G. J., J. W. Teng, and X. K. Zhang (2007), The crustal structure of western Shandong and the high velocity body in the crust, *Chin. J. Geophys.*, *50*(5), 1480–1487, doi:10.1002/cjg2.1148.

Wang, S., X. Zhang, B. Liu, S. Pan, and Y. Hai (2005), Sounding research on deep crust tectonic in midwest segment and its adjacent region of Zhangjiakou-Bohai seismic zone, *J. Geod. Geodyn.*, *25*(3), 110–115.

Wang, S. J., X. K. Zhang, B. F. Liu, S. Z. Pan, and Y. Hai (2005), Souding research on deep crust tectonic in midwest segment and its adjacent region of Zhangjiakou-Bohai seismic zone, *J. Geod. Geodyn.*, *25*(3), 110–115.

Wang, S. J., X. K. Zhang, C. K. Zhang, F. Y. Wang, J. R. Zhao, J. S. Zhang, B. F. Liu, S. Z. Pan, and Y. J. Guo (2007), 2D crystal structures alone Wuqing-Beijing-Chicheng deep seismic sounding profile, *Chin. J. Geophys.*, *50*(6), 1525–1534, doi:10.1002/cjg2.1172.

Wang, S. J., F. Y. Wang, J. S. Zhang, S. X. Jia, C. K. Zhang, J. R. Zhao, and B. F. Liu (2014), The P-wave velocity structure of the lithosphere of the North China Craton—Results from the Wendeng-Alxa left banner deep seismic sounding profile, *Sci. China Earth Sci.*, *57*(9), 2053–2063, doi:10.1007/s11430-014-4903-7.

Wei, Z. G., L. Chen, Z. W. Li, L. Yuan, and J. Li (2016), Regional variation in Moho depth and Poisson's ratio beneath eastern China and its tectonic implications, *J. Asian Earth Sci.*, *115*(1), 308–320, doi:10.1016/j.jseaes.2015.10.010.

Wu, F. Y, J. Q. Lin, S. A. Wilde, X. O. Zhang, and J. H. Yang (2005a), Nature and significance of the Early Cretaceous giant igneous event in eastern China, *Earth Planet. Sci. Lett.*, *233*(12), 103–119, doi:10.1016/j.epsl.2005.02.019.

Wu, F. Y, G. C. Zhao, S. A. Wilde, and D. Y. Sun (2005b), Nd isotopic constraints on crustal formation in the North China Craton, *J. Asian Earth Sci.*, *24*(5), 523–545, doi:10.1016/j.jseaes.2003.10.011.

Xu, T., Z. J. Zhang, X. B. Tian, B. F. Liu, Z. M. Bai, Q. T. Lu, and J. W. Teng (2014), Crustal structure beneath the Middle-Lower Yangtze metallogenic belt and its surrounding areas: Constraints from active source seismic experiment along the Lixin to Yixing profile in East China, *Acta Petrologica Sin.*, *30*(4), 918–930, doi:1000-0569/2014/030(04)-0918-30.

Xu, W. L., S. Gao, Q. H. Wang, D. Y. Wang, and Y. S. Liu (2006), Mesozoic crustal thickening of the eastern North China craton: Evidence from eclogite xenoliths and petrologic implications, *Geology*, *34*(9), 721–724, doi:10.1130/g22551.1.

Xu, X. S, S. Y. O'Reilly, W. L. Griffin, and X. M. Zhang (2000), Genesis of young lithospheric mantle in Southeastern China: An LAM-ICPMS trace element study, *J. Petrol.*, *41*(1), 111–148, doi:10.1093/petrology/41.1.111.

Yegorova, T., U. Bayer, H. Thybo, Y. Maystrenko, M. Scheck-Wenderoth, and S. B. Lyngsie (2007), Gravity signals from the lithosphere in the Central European Basin System, *Tectonophysics*, *429*(1–2), 133–163, doi:10.1016/j.tecto.2006.10.002.

Youssof, M., H. Thybo, I. M. Artemieva, and A. Levander (2013), Moho depth and crustal composition in Southern Africa, *Tectonophysics*, *609*, 267–287, doi:10.1016/j.tecto.2013.09.001.

Yu, C. Q., W. P. Chen, J. Y. Ning, K. Tao, T. L. Tseng, X. D. Fang, Y. S. Chen, and R. D. van der Hilst (2012), Thick crust beneath the Ordos plateau: Implications for instability of the North China craton, *Earth Planet. Sci. Lett.*, *357–358*, 366–375, doi:10.1016/j.epsl.2012.09.027.

Zhang, C. K., X. K. Zhang, Y. J. Gai, Z. P. Zhu, J. S. Zhang, and H. Ruan (1997), A study of crust and upper mantle structure on Wenan-Weixian-Qanharyouyizhongqi profile, *North China Earthquake Sci.*, *15*(3), 18–28.

Zhang, C. K., J. R. Zhao, and Q. F. Ren (1994), Study on crust and upper mantle structure in north Henan and its surroundings, *Seismol. Geol.*, *16*(3), 243–253.

Zhang, J. S., Z. P. Zhu, X. K. Zhang, C. K. Zhang, Y. J. Gai, and W. Y. Nie (1997), The seismic velocity structure of crust and upper mantle and deep structure feature in north Shanxi Plateau, *Seismol. Geol.*, *19*(3), 220–226.

Zhang, Q., Y. Wang, G. Q. Pan, C. D. Li, and W. J. Jin (2008), Sources of granites: Some crucial questions on granite study (4), *Acta Petrologica Sinica*, *24*(6), 1193–1204.

Zhang, S. W., S. X. Zhang, R. Y. Tang, Z. H. Liang, J. M. Tang, J. D. Liu, and J. J. Song (1988), Interpretation of the Fuliji-Fengxian DSS Profile in Xiayangzi Region, *Acta Geophys. Sin.*, *31*(6), 637–648.

Zhang, X. K., C. Y. Wang, G. D. Liu, J. L. Song, L. L. Luo, T. Wu, and J. C. Wu (1996), Fine crustal structure in Yanqing-Huailai region by deep seismic reflection profiling, *Acta Geophys. Sin.*, *39*(3), 356–364.

Zhang, Y. Q., J. W. Teng, Q. S. Wang, F. Y. Wang, and Q. T. Lü (2014), Composition model of the crust beneath the Ordos basin and the Yinshan mountains in China, based on seismic velocity, heat flow and gravity data, *Tectonophysics*, *634*, 246–256, doi:10.1016/j.tecto.2014.07.006.

Zhang, Z. J., L. Q. Yang, J. W. Teng, and J. Badal (2011), An overview of the earth crust under China, *Earth Sci. Rev.*, *104*(1–3), 143–166, doi:10.1016/j.earscirev.2010.10.003.

Zhao, G. C., and M. G. Zhai (2013), Lithotectonic elements of Precambrian basement in the North China Craton: Review and tectonic implications, *Gondwana Res.*, *23*(4), 1207–1240, doi:10.1016/j.gr.2012.08.016.

Zhao, J. R., X. K. Zhang, C. K. Zhang, Z. P. Zhu, Q. F. Ren, and J. S. Zhang (1999), The crust-mantle tectonic and velocity structure characteristics Xianghe-Beijing-Zhulu and its adjacent areas, *Seismol. Geol.*, *21*, 29–36.

Zhao, J. R., X. K. Zhang, C. K. Zhang, J. S. Zhang, B. F. Liu, Q. F. Ren, S. Z. Pan, and Y. Hai (2005), The heterogeneous characteristics of crust-mantle structures and the seismic activities in the northwest Beijing region, *Acta Seismol. Sin.*, *27*(2), 119–127, doi:10.1007/s11589-005-0059-z.

Zhao, J. R., X. K. Zhang, C. K. Zhang, J. S. Zhang, B. F. Liu, and S. Z. Pan (2006), Features of deep crustal structure beneath the Wutai mountain area of Shanxi province, *Chin. J. Geophys.*, *49*(1), 123–129, doi:10.1002/cjg2.818.

Zheng, J. P., W. L. Griffin, S. Y. O'Reilly, C. M. Yu, H. F. Zhang, N. Pearson, and M. Zhang (2007), Mechanism and timing of lithospheric modification and replacement beneath the eastern North China Craton: Peridotitic xenoliths from the 100 Ma Fuxin basalts and a regional synthesis, *Geochim. Cosmochim. Acta*, *71*(21), 5203–5225, doi:10.1016/j.gca.2007.07.028.

Zheng, J. P., S. Y. O'Reilly, W. L. Griffin, F. X. Lu, and M. Zhang (1998), Nature and evolution of Cenozoic lithospheric mantle beneath Shandong Peninsula, Sino-Korean Craton, Eastern China, *Int. Geol. Rev.*, *40*(6), 471–499, doi:10.1080/00206819809465220.

Zheng, Y., and J. W. Teng (1989), The structure of the crust and upper mantle in the Suixian-Maanshan zone and some characteristics of the southern part of the Tan-Lu tectonic belt, *Acta Geophys. Sin.*, *32*(6), 649–659.

Zheng, Y. F., W. J. Xiao and G. C. Zhao (2013), Introduction to tectonics of China, *Gondwana Res.*, *23*(4), 1189–1206, doi:10.1016/j.gr.2012.10.001.